# Sivers and Boer-Mulders functions in Light-Cone Quark Models

Barbara Pasquini*

*Dipartimento di Fisica Nucleare e Teorica,*
*Università degli Studi di Pavia, and*

*Istituto Nazionale di Fisica Nucleare,*
*Sezione di Pavia, I-27100 Pavia, Italy*

Feng Yuan†

*Nuclear Science Division, Lawrence Berkeley National Laboratory,Berkeley, CA 94720 and*

*RIKEN BNL Research Center, Building 510A,*
*Brookhaven National Laboratory, Upton, NY 11973*

## Abstract

Results for the naive-time-reversal-odd quark distributions in a light-cone quark model are presented. The final-state interaction effects are generated via single-gluon exchange mechanism. The formalism of light-cone wave functions is used to derive general expressions in terms of overlap of wave-function amplitudes describing the different orbital angular momentum components of the nucleon. In particular, the model predictions show a dominant contribution from $S$- and $P$-wave interference in the Sivers function and a significant contribution also from the interference of $P$ and $D$ waves in the Boer-Mulders function. The favourable comparison with existing phenomenological parametrizations motivates further applications to describe azimuthal asymmetries in hadronic reactions.

PACS numbers: 12.39.ki,13.85.Qk,13.88.+e

*pasquini@pv.infn.it
†fyuan@lbl.gov

## I. INTRODUCTION

Transverse momentum dependent parton distributions (TMDs), as an important extension to the usual Feynman parton distributions, have attracted much attention in hadronic physics from both experiment and theory sides. Various hadronic processes have been used and proposed to study these distributions [1–21]. Together with the generalized parton distributions (GPDs) (for reviews, see [22–26]), TMDs shall lead us to a comprehensive picture of parton distributions inside the nucleon, in particular, in a three-dimension fashion.

Phenomenologically, in order to extract these distribution functions from experiments, we have to ensure that the QCD factorization applies in the associated processes. These issues have been extensively discussed in the last few years, and the relevant factorization theorem has been built up for a number of semi-inclusive processes, such as semi-inclusive hadron production in deep inelastic scattering and low transverse momentum Drell-Yan lepton pair production in hadronic collisions [27–29]. In the last few years, there has also been a remarkable experimental progress on experimental measurements (see Ref. [21] and references therein). More importantly, the proposed future experiments shall provide more constraints on these distribution functions.

Meanwhile, reasonable model calculations of these transverse momentum dependent parton distributions have been proposed [30–63]. These calculations promoted our understanding of the nucleon structure, and have been playing very important role as a first step to describe the experimental observations of the associated phenomena. In particular, these models provide us an intuitive way to connect the physical observables and the key input for the nucleon structure model, such as the quark spin and orbital angular momentum contributions to the proton spin.

Transverse momentum dependent quark distributions are defined through the following quark-density matrix

$$\mathcal{M}(x, \boldsymbol{k}_\perp) = \int \frac{d\xi^- d^2\boldsymbol{\xi}_\perp}{(2\pi)^3} e^{-ik\cdot\xi} \langle PS|\bar{\psi}(\xi)\mathcal{L}_\xi^\dagger \mathcal{L}_0 \psi(0)|PS\rangle \ , \tag{1}$$

where $x$ and $\boldsymbol{k}_\perp$ are the longitudinal momentum fraction and transverse momentum carried by the quark, respectively. Nucleon's momentum $P$ is dominated by the plus component $P^+ = (P^0 + P^z)/\sqrt{2}$, and $S$ represents the polarization vector. In the above equation, the gauge link $\mathcal{L}$ is very important to retain the gauge invariance and leading to nonzero naive-time-reversal-odd (T-odd) quark distributions. Among the leading order eight TMD quark distributions, six of them are called the naive-time-reversal even (T-even), whereas the rest two belong to the T-odd distributions. One is the so-called quark Sivers function, which describes the quark transverse momentum distribution correlated to the transverse polarization vector of the nucleon. The other is the so-called Boer-Mulders function, and usually interpreted as the transverse momentum correlated with the quark transverse polarization. Both quark distributions contribute to the azimuthal asymmetries in hadronic reaction processes.

In Ref. [44], we have calculated the T-even quark distributions in a light-cone quark model, extending previous works on the parton distribution functions (PDFs) [35], the GPDs [64–67], and nucleon form factors [68]. Such a model, based on the light-cone wave-function (LCWF) overlap representation, is able to capture the relevant information on the three-quark contribution to different observables. These calculations are well suited to illustrate the relevance of the different orbital angular momentum components of the nucleon wave

function, and provide an intuitive picture for the physical meaning of the TMD quark distributions. Moreover, they can be regarded as initial input for phenomenological studies for the semi-inclusive processes where TMD quark distributions play a very important role [70].

In this paper, we extend these works to the T-odd quark distributions. The unique feature for the latter distributions is the final/initial state interaction effects. Without these effects, the T-odd parton distributions would vanish. In the model calculation, these interactions are calculated by taking into account the one-gluon exchange mechanism between the struck quark and the nucleon spectators described by (real) LCWFs. This approach is complementary to a recent work [71] where the rescattering effects are incorporated in augmented LCWFs containing an imaginary phase which depends on the choice of advanced or retarded boundary condition for the gauge potential in the light-cone gauge. Recently, there has also been interesting study to go beyond the one-gluon exchange approximation, by resumming all order contributions [61, 62].

The rest of the paper is organized as follows. In Sec. II, we briefly introduce the light-cone quark model, explaining its physical content and giving results for the light-cone wave-function amplitudes describing the different orbital angular momentum components of the nucleon state. In Sec. III, we derive the quark Sivers function. We present a general formalism in terms of overlap of light-cone wave-function amplitudes, and then apply it to a specific light-cone quark model wave function. The corresponding formalism for the Boer-Mulders function is described in Sec. IV. The model results for the T-odd distributions are presented in Sec. V and compared to different phenomenological parametrizations. Finally, we conclude with a section summarizing our findings.

## II. LIGHT-CONE AMPLITUDES IN A CONSTITUENT QUARK MODEL

The wave-function amplitudes in light-cone quantization for the three-quark Fock state of the nucleon has been studied extensively in the literature [69]. According to the total quark orbital angular momentum projection, these wave-function amplitudes are classified into $l_z = 0$, $l_z = 1$, $l_z = 2$, $l_z = -1$ components for total spin $+1/2$ of nucleon, i.e.,

$$|P\uparrow\rangle_{uud} = |P\uparrow\rangle_{uud}^{l_z=0} + |P\uparrow\rangle_{uud}^{l_z=1} + |P\uparrow\rangle_{uud}^{l_z=-1} + |P\uparrow\rangle_{uud}^{l_z=2}. \tag{2}$$

For completeness, we list the parametrization for these wave-function amplitudes following Refs. [72–74]:

$$\begin{aligned}
|P\uparrow\rangle_{uud}^{l_z=0} &= \int d[1]d[2]d[3] \left(\psi_{uud}^{(1)}(1,2,3) + i\epsilon^{\alpha\beta}k_{1\alpha}k_{2\beta}\psi_{uud}^{(2)}(1,2,3)\right) \\
&\quad \times \frac{\epsilon^{ijk}}{\sqrt{6}} b_{i\uparrow}^{\dagger\,u}(1) \left(b_{j\downarrow}^{\dagger\,u}(2) b_{k\uparrow}^{\dagger\,d}(3) - b_{j\downarrow}^{\dagger\,d}(2) b_{k\uparrow}^{\dagger\,u}(3)\right)|0\rangle \ , \qquad (3) \\
|P\uparrow\rangle_{uud}^{l_z=1} &= \int d[1]d[2]d[3] \left(k_{1\perp}^{+}\psi_{uud}^{(3)}(1,2,3) + k_{2\perp}^{+}\psi_{uud}^{(4)}(1,2,3)\right) \\
&\quad \times \frac{\epsilon^{ijk}}{\sqrt{6}} \left(b_{i\uparrow}^{\dagger\,u}(1) b_{j\downarrow}^{\dagger\,u}(2) b_{k\downarrow}^{\dagger\,d}(3) - b_{i\uparrow}^{\dagger\,d}(1) b_{j\downarrow}^{\dagger\,u}(2) b_{k\downarrow}^{\dagger\,u}(3)\right)|0\rangle \ , \qquad (4) \\
|P\uparrow\rangle_{uud}^{l_z=-1} &= \int d[1]d[2]d[3] \ k_{2\perp}^{-}\psi_{uud}^{(5)}(1,2,3) \\
&\quad \times \frac{\epsilon^{ijk}}{\sqrt{6}} b_{i\uparrow}^{\dagger\,u}(1) \left(b_{j\uparrow}^{\dagger\,u}(2) b_{k\uparrow}^{\dagger\,d}(3) - b_{j\uparrow}^{\dagger\,d}(2) b_{k\uparrow}^{\dagger\,u}(3)\right)|0\rangle \ , \qquad (5)
\end{aligned}$$

$$|P\uparrow\rangle^{l_z=2}_{uud} = \int d[1]d[2]d[3]\ k^+_{1\perp}k^+_{3\perp}\psi^{(6)}_{uud}(1,2,3)$$
$$\times\frac{\epsilon^{ijk}}{\sqrt{6}}b^{\dagger\,u}_{i\downarrow}(1)\left(b^{\dagger\,d}_{j\downarrow}(2)b^{\dagger\,u}_{k\downarrow}(3) - b^{\dagger\,u}_{j\downarrow}(2)d^{\dagger}_{k\downarrow}(3)\right)|0\rangle\ , \tag{6}$$

where $\alpha,\beta = 1,2$ are transverse indexes and $k^{\pm}_{i\perp} = k^x_i \pm k^y_i$. In Eqs. (3)-(6) the integration measures are defined as

$$d[1]d[2]d[3] = \frac{dx_1dx_2dx_3}{\sqrt{x_1x_2x_3}}\delta\left(1-\sum_{i=1}^{3}x_i\right)\frac{d^2\boldsymbol{k}_{1\perp}d^2\boldsymbol{k}_{2\perp}d^2\boldsymbol{k}_{3\perp}}{[2(2\pi^3)]^2}\delta\left(\sum_{i=1}^{3}\boldsymbol{k}_{i\perp}\right), \tag{7}$$

with $x_i$ the fraction of the longitudinal nucleon momentum carried by the quarks, and $\boldsymbol{k}_{i\perp}$ their transverse momenta. Furthermore, $b^{\dagger\,q}_{i,\lambda}$ and $b^{q}_{i,\lambda}$ are creation and annihilation operators of a quark with flavour $q$, helicity $\lambda$ and color $i$, respectively. In the following, we will describe the above light-cone wave-function amplitudes in a light-cone constituent quark model (CQM) following Ref. [44]. Working in the so-called "uds" basis [75, 76] the proton state is given in terms of a completely symmetrized wave function of the form

$$|P\uparrow\rangle = |P\uparrow\rangle_{uud} + |P\uparrow\rangle_{udu} + |P\uparrow\rangle_{duu}\,. \tag{8}$$

In this symmetrization, the state $|P\uparrow\rangle_{udu}$ is obtained from $|P\uparrow\rangle_{uud}$ by interchanging the second and third spin and space coordinates as well as the indicated quark type, with a similar interchange of the first and third coordinates for $|P\uparrow\rangle_{duu}$.

Following the derivation outlined in Ref. [64], we find that the *uud* component of the light-cone state of the proton can be written as

$$|P,\Lambda\rangle_{uud} = \sum_{\lambda_i,c_i}\int d[1]d[2]d[3]\Psi^{\Lambda,[f]}_{uud}(\{x_i,\boldsymbol{k}_{i\perp};\lambda_i\})\frac{\epsilon^{ijk}}{\sqrt{6}}u^{\dagger}_{i,\lambda_1}(1)u^{\dagger}_{j,\lambda_2}(2)d^{\dagger}_{k,\lambda_3}(3)|0\rangle\,. \tag{9}$$

In Eq. (9), assuming SU(6) spin-flavor symmetry, we can factorize the LCWF $\Psi^{\Lambda,[f]}_{uud}(\{x_i,\boldsymbol{k}_{i\perp};\lambda_i\})$ in a momentum-dependent wave function and a spin-dependent part, i.e.,

$$\Psi^{\Lambda,[f]}_{uud}(\{x_i,\boldsymbol{k}_{i\perp};\lambda_i\}) = \tilde{\psi}(\{x_i,\boldsymbol{k}_{i\perp}\})\frac{1}{\sqrt{3}}\tilde{\Phi}_{\Lambda}(\lambda_1,\lambda_2,\lambda_3). \tag{10}$$

In the above equation the momentum-dependent function is given by

$$\tilde{\psi}(\{x_i,\boldsymbol{k}_{i\perp}\}) = 2(2\pi)^3\left[\frac{1}{M_0}\frac{\omega_1\omega_2\omega_3}{x_1x_2x_3}\right]^{1/2}\psi(\{x_i,\boldsymbol{k}_{i\perp}\}), \tag{11}$$

where $\psi(\{x_i,\boldsymbol{k}_{i\perp}\})$ is symmetric under exchange of the momenta of any quark pairs and is spherically symmetric, $\omega_i$ is the free-quark energy, and $M_0 = \sum_i\omega_i$ is the mass of the non-interacting three-quark system. The spin-dependent part in Eq. (10) is given by

$$\tilde{\Phi}_{\Lambda}(\lambda_1,\lambda_2,\lambda_3) = \sum_{\mu_1\mu_2\mu_3}\langle 1/2,\mu_1;1/2,\mu_2|1,\mu_1+\mu_2\rangle\langle 1,\mu_1+\mu_2;1/2,\mu_3|1/2,\Lambda\rangle$$
$$\times D^{1/2*}_{\mu_1\lambda_1}(R_{cf}(x_1,\boldsymbol{k}_{1\perp}))D^{1/2*}_{\mu_2\lambda_2}(R_{cf}(x_2,\boldsymbol{k}_{2\perp}))D^{1/2*}_{\mu_3\lambda_3}(R_{cf}(x_3,\boldsymbol{k}_{3\perp})). \tag{12}$$

In Eq. (12), $D^{1/2}_{\lambda\mu}(R_{cf}(x,\boldsymbol{k}_\perp))$ is the matrix element of the Melosh rotation $R_{cf}$ [77]

$$D^{1/2}_{\lambda\mu}(R_{cf}(x,\boldsymbol{k}_\perp)) = \langle\lambda|R_{cf}(x,\boldsymbol{k}_\perp)|\mu\rangle$$
$$= \langle\lambda|\frac{m+xM_0-i\boldsymbol{\sigma}\cdot(\hat{\boldsymbol{z}}\times\boldsymbol{k}_\perp)}{\sqrt{(m+xM_0)^2+\boldsymbol{k}_\perp^2}}|\mu\rangle. \tag{13}$$

The Melosh rotation corresponds to the unitary transformation which converts the Pauli spinors of the quark in the nucleon rest-frame to the light-front spinor. In particular, the spin wave function of Eq. (12) is obtained from the transformation of the non-relativistic spin wave function with zero orbital angular momentum component. The relativistic spin effects are immediately evident in the presence of the spin-flip term $i\boldsymbol{\sigma}\cdot(\hat{\boldsymbol{z}}\times\boldsymbol{k}_\perp)$ in Eq. (13). Such a term generates non-zero orbital angular momentum, and, as a consequence of total angular momentum conservation, total quark helicity different from the nucleon helicity. Making explicit the dependence on the quark helicities, the spin wave function of Eq. (12) takes the following values:

$$\tilde{\Phi}_\uparrow(\uparrow,\uparrow,\downarrow) = \prod_i \frac{1}{\sqrt{N(x_i,\boldsymbol{k}_{i\perp})}}\frac{1}{\sqrt{6}}(2a_1a_2a_3 + a_1k_2^-k_3^+ + a_2k_1^-k_3^+), \tag{14}$$

$$\tilde{\Phi}_\uparrow(\uparrow,\downarrow,\uparrow) = \prod_i \frac{1}{\sqrt{N(x_i,\boldsymbol{k}_{i\perp})}}\frac{1}{\sqrt{6}}(-a_1a_2a_3 + a_3k_1^-k_2^+ - 2a_1k_2^+k_3^-), \tag{15}$$

$$\tilde{\Phi}_\uparrow(\downarrow,\uparrow,\uparrow) = \prod_i \frac{1}{\sqrt{N(x_i,\boldsymbol{k}_{i\perp})}}\frac{1}{\sqrt{6}}(-a_1a_2a_3 + a_3k_1^+k_2^- - 2a_2k_1^+k_3^-), \tag{16}$$

$$\tilde{\Phi}_\uparrow(\uparrow,\downarrow,\downarrow) = \prod_i \frac{1}{\sqrt{N(x_i,\boldsymbol{k}_{i\perp})}}\frac{1}{\sqrt{6}}(a_1a_2k_3^+ - k_1^-k_2^+k_3^+ - 2a_1a_3k_2^+), \tag{17}$$

$$\tilde{\Phi}_\uparrow(\downarrow,\uparrow,\downarrow) = \prod_i \frac{1}{\sqrt{N(x_i,\boldsymbol{k}_{i\perp})}}\frac{1}{\sqrt{6}}(-k_1^+k_2^-k_3^+ + a_1a_2k_3^+ - 2a_2a_3k_1^+), \tag{18}$$

$$\tilde{\Phi}_\uparrow(\downarrow,\downarrow,\uparrow) = \prod_i \frac{1}{\sqrt{N(x_i,\boldsymbol{k}_{i\perp})}}\frac{1}{\sqrt{6}}(a_2a_3k_1^+ + a_1a_3k_2^+ + 2k_1^+k_2^+k_3^-), \tag{19}$$

$$\tilde{\Phi}_\uparrow(\uparrow,\uparrow,\uparrow) = \prod_i \frac{1}{\sqrt{N(x_i,\boldsymbol{k}_{i\perp})}}\frac{1}{\sqrt{6}}(-a_1a_3k_2^- - a_2a_3k_1^- + 2a_1a_2k_3^-), \tag{20}$$

$$\tilde{\Phi}_\uparrow(\downarrow,\downarrow,\downarrow) = \prod_i \frac{1}{\sqrt{N(x_i,\boldsymbol{k}_{i\perp})}}\frac{1}{\sqrt{6}}(-a_2k_1^+k_3^+ - a_1k_2^+k_3^+ + 2a_3k_1^+k_2^+), \tag{21}$$

where $a_i = (m + x_iM_0)$, and $N(x_i,\boldsymbol{k}_{i\perp}) = [(m+x_iM_0)^2 + \boldsymbol{k}_{i\perp}^2]$.

Taking into account the quark-helicity dependence in Eqs. (14)-(21), the nucleon state can be mapped out into the different angular momentum components. After straightforward algebra, one finds the following representation for the nucleon wave-function amplitudes in the light-cone CQM

$$\psi^{(1)}(1,2,3) = \tilde{\psi}(\{x_i,\boldsymbol{k}_{i\perp}\})$$
$$\times\prod_i \frac{1}{\sqrt{N(x_i,\boldsymbol{k}_{i\perp})}}\frac{1}{\sqrt{3}}(-a_1a_2a_3 + a_3\boldsymbol{k}_{1\perp}\cdot\boldsymbol{k}_{2\perp} + 2a_1\boldsymbol{k}_{1\perp}\cdot\boldsymbol{k}_{2\perp} + 2a_1\boldsymbol{k}_{2\perp}^2), \tag{22}$$

$$\psi^{(2)}(1,2,3) = \tilde{\psi}(\{x_i,\boldsymbol{k}_{i\perp}\})\prod_i \frac{1}{\sqrt{N(x_i,\boldsymbol{k}_{i\perp})}}\frac{1}{\sqrt{3}}(a_3 + 2a_1), \tag{23}$$

$$\psi^{(3)}(1,2,3) = -\tilde{\psi}(\{x_i, \boldsymbol{k}_{i\perp}\}) \prod_i \frac{1}{\sqrt{N(x_i, \boldsymbol{k}_{i\perp})}} \frac{1}{\sqrt{3}} (a_1 a_2 + \boldsymbol{k}_{2\perp}^2), \tag{24}$$

$$\psi^{(4)}(1,2,3) = -\tilde{\psi}(\{x_i, \boldsymbol{k}_{i\perp}\}) \prod_i \frac{1}{\sqrt{N(x_i, \boldsymbol{k}_{i\perp})}} \frac{1}{\sqrt{3}} (a_1 a_2 + 2a_3 a_1 - \boldsymbol{k}_{1\perp}^2 - 2\boldsymbol{k}_{1\perp} \cdot \boldsymbol{k}_{2\perp}), \tag{25}$$

$$\psi^{(5)}(1,2,3) = \tilde{\psi}(\{x_i, \boldsymbol{k}_{i\perp}\}) \prod_i \frac{1}{\sqrt{N(x_i, \boldsymbol{k}_{i\perp})}} \frac{1}{\sqrt{3}} (a_1 a_3), \tag{26}$$

$$\psi^{(6)}(1,2,3) = \tilde{\psi}(\{x_i, \boldsymbol{k}_{i\perp}\}) \prod_i \frac{1}{\sqrt{N(x_i, \boldsymbol{k}_{i\perp})}} \frac{1}{\sqrt{3}} a_2. \tag{27}$$

Notice that the results in Eqs. (22)-(27) follow from the spin and orbital angular momentum structure generated from the Melosh rotations, and are independent on the functional form of the momentum-dependent wave function.

## III. SIVERS FUNCTION

The quark Sivers function can be calculated from the following definition

$$f_{1T}^{\perp}(x, \boldsymbol{k}_\perp^2) = -i(k^x + ik^y) \frac{M}{2\boldsymbol{k}_\perp^2} \int \frac{d\xi^- d^2\boldsymbol{\xi}_\perp}{(2\pi)^3} e^{-i(\xi^- k^+ - \boldsymbol{\xi}_\perp \cdot \boldsymbol{k}_\perp)} \langle P \uparrow | \bar{\psi}(\xi^-, \boldsymbol{\xi}_\perp) \mathcal{L}_\xi^\dagger \gamma^+ \mathcal{L}_0 \psi(0) | P \downarrow \rangle \ . \tag{28}$$

As we discussed in the Introduction, the gauge link is crucial to obtain a non-zero Sivers function. In the covariant gauge, the gauge link can be reduced to the light-cone gauge link[1]. According to the light-cone wave function model, in the following calculations we choose the light-cone gauge $A^+ = 0$, where the gauge link reduces to a transverse gauge link at $\xi^- = \infty$, i.e.,

$$\mathcal{L}_\xi|_{A^+=0} = \mathcal{P} \exp\left( -ig \int_{\boldsymbol{\xi}_\perp}^{\infty} \mathrm{d}^2 \boldsymbol{\zeta}_\perp \cdot \boldsymbol{A}_\perp(\xi^- = \infty, \boldsymbol{\zeta}_\perp) \right) \ . \tag{29}$$

In the Sivers function of Eq. (28), we will expand the above gauge link to take into account the contribution from the one-gluon exchange diagram. Furthermore, in the light-cone gauge the gluon propagator takes the following form

$$d^{\mu\nu}(q) = -g^{\mu\nu} + \frac{n^\mu q^\nu + n^\nu q^\mu}{[n \cdot q]} \ , \tag{30}$$

where $n$ is the light-like vector $n^2 = 0$ and $n \cdot q = q^+$. The gluon propagator has a light-cone singularity, as can be seen from the above equation. We will adopt the principal-value prescription to regulate this singularity. We have also checked that the final results do not

[1] An off-light-cone gauge link has to be used to regulate the light-cone singularities for higher-order calculations. In this paper, we will not encounter this singularity. Therefore, we will simply adopt the gauge link along the light-cone direction in covariant gauge and the transverse gauge link at spatial infinity in light-cone gauge.

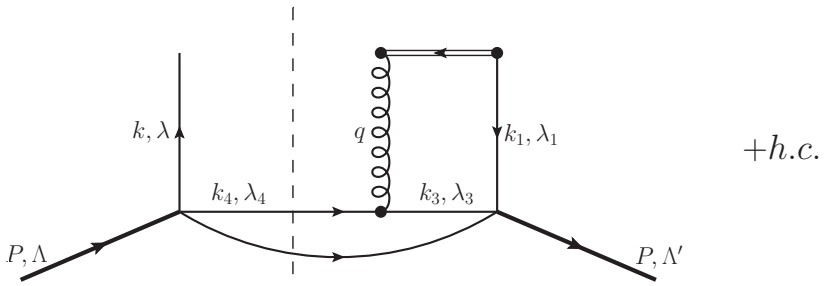


FIG. 1. The leading contribution from the one-gluon exchange mechanism to the T-odd distribution functions.

depend on the prescription.[2] Under this prescription, there is no phase contribution from the above propagator. However, the transverse gauge link expansion, when combining with the $n^-\boldsymbol{q}_\perp/n\cdot q$ factor of the above equation, leads to the following expression

$$\frac{e^{iq^+\infty}}{q^+} = i\pi\delta(q^+)\ . \tag{31}$$

This contribution provides the phase needed to generate a non-zero Sivers function. The dominance in the gluon propagator of the $n^-\boldsymbol{q}_\perp/n\cdot q$, with the $\perp$ index coming from the contraction with the transverse gauge link, also simplifies the interactions between the quark fields, since the quark scattering conserves the helicity.

Finally, we obtain the following expression for the quark Sivers function

$$f_{1T}^{\perp q}(x,\boldsymbol{k}_\perp^2) = -g^2\frac{k^x+ik^y}{\boldsymbol{k}_\perp^2}\frac{M}{2}\frac{1}{(2\pi)^{11}}\frac{1}{\sqrt{(2k^+)(2k_1^+)}}\int\frac{\mathrm{d}k_3^+\mathrm{d}^2\,\boldsymbol{k}_{3\perp}}{\sqrt{(2k_3^+)(2k_4^+)}}\int\mathrm{d}^2\,\boldsymbol{q}_\perp$$
$$\times\Big\{\frac{1}{\boldsymbol{q}_\perp^2}\sum_{\lambda_1,\lambda_3}\sum_f\sum_{i.j}\sum_{k,l}T^a_{ij}T^b_{kl}\delta_{ab}\langle P\uparrow|b^{\dagger\,q}_{i\lambda_1}(k_1)b^q_{j\lambda_1}(k)b^{\dagger\,f}_{k\lambda_3}(k_3)b^f_{l\lambda_3}(k_4)|P\downarrow\rangle\Big\}, \tag{32}$$

where the quark momenta are defined as $k_1 = k - q$, $k_4 = k_3 - q$, $T^a$ is the $SU_c(6)$ Gell-Mann matrix and $g$ is the gluon coupling with the quark field. Equation (32) corresponds to the diagrams in Fig. 1 with $\lambda = \lambda_1$ and $\lambda_4 = \lambda_3$, for the helicity of the interacting and spectator quarks, respectively, and $\Lambda = -\Lambda'$ for the helicity of the nucleon in the initial and final states. A few comments are in order to explain the above derivations. First, we have made an approximation for the interaction vertex between the gauge field from the gauge link and the quark fields in the proton wave function, by the covariant interaction form. In principle, we shall use the light-cone time-order perturbation theory to describe this interaction. However, we expect the modification being beyond the approximation we made in modelling the light-cone wave function itself. Nevertheless, it will be interesting to check how large these effects would be. Second, we used the perturbation theory to calculate the final-state interaction effects. For numerical estimate, we choose a reasonable value for the strong coupling constant (see Sec. V). Meanwhile, we notice it may be not appropriate

[2] For example, if we choose the so-called advanced boundary condition for the gauge potential, the transverse gauge link becomes unit, whereas the above gluon propagator generates phases which allow to recover the previous results with the principal-value prescription.

to use a perturbative coupling for this non-perturbative calculations. We regarded this as an important theoretical uncertainty, which exists in all model calculations of the Sivers function.

As we discussed, in Eq. (32) the quark helicity is conserved. On the other side, the hadron helicity flips from the initial to the final state. As a consequence, non-zero results for the Sivers function can be obtained only with a transfer of one unit of orbital angular momentum between the initial and the final nucleon states.
Inserting in Eq. (32) the light-cone wave-function amplitude decomposition of the nucleon state introduced in Sec. II, one finds the following results in terms of the amplitudes $\psi^{(i)}$

$$f_{1T}^{\perp q}(x, \boldsymbol{k}_\perp^2) = -\frac{2}{3} g^2 M \frac{k^x + ik^y}{\boldsymbol{k}_\perp^2} \int \frac{\mathrm{d}^2 \boldsymbol{q}_\perp}{(2\pi)^2} \frac{1}{\boldsymbol{q}_\perp^2} \int \mathrm{d}x' \int \mathrm{d}^2 \boldsymbol{t}'_\perp \int d[1]d[2]d[3] \sqrt{x_1 x_2 x_3}\, \mathcal{F}^{\perp q}. \tag{33}$$

The function $\mathcal{F}^{\perp q}$ for $u$ quark is given by

$$\mathcal{F}^{\perp u} = A^{(1,2)}\phi^{(3,4)}(1,2,3) - A^{(3,4)}\phi^{(1,2)}(1,2,3) - A^{(5)}\phi^{(6)}(1,2,3) + A^{(6)}\phi^{(5)}(1,2,3), \tag{34}$$

where

$$\begin{aligned}
\phi^{(1,2)}(1,2,3) &= \psi^{(1)}(1,2,3) - i(k_1^x k_2^y - k_1^y k_2^x)\psi^{(2)}(1,2,3), \\
\phi^{(3,4)}(1,2,3) &= k_1^- \psi^{(3)}(1,2,3) + k_2^- \psi^{(4)}(1,2,3), \\
\phi^{(5)}(1,2,3) &= k_2^+ \psi^{(5)}(1,2,3) - k_3^+ \psi^{(5)}(1,3,2), \\
\phi^{(6)}(1,2,3) &= k_1^- k_3^- \psi^{(6)}(1,2,3) - k_1^- k_2^- \psi^{(6)}(1,3,2).
\end{aligned} \tag{35}$$

The functions $A$ in Eq. (34) are defined through

$$\begin{aligned}
A^{(1,2)} = {} & \delta^3(k-k_1)\Big[\delta^3(t'-k_2)\phi^{(1,2)*}(\hat{2},1'',3) + \delta^3(t'-k_3)\phi^{(1,2)*}(2,1'',\hat{3})\Big] \\
& + \delta^3(k-k_2)\Big[\delta^3(t'-k_1)\Big(2\phi^{(1,2)*}(2'',\hat{1},3) + \phi^{(1,2)*}(3,\hat{1},2'')\Big) \\
& + \delta^3(t'-k_3)\Big(2\phi^{(1,2)*}(2'',1,\hat{3}) + \phi^{(1,2)*}(\hat{3},1,2'')\Big)\Big] \\
& + \delta^3(k-k_3)\Big[\delta^3(t'-k_1)\Big(\phi^{(1,2)*}(2,\hat{1},3'') + \phi^{(1,2)*}(3'',\hat{1},2)\Big) \\
& + \delta^3(t'-k_2)\Big(\phi^{(1,2)*}(\hat{2},1,3'') + \phi^{(1,2)*}(3'',1,\hat{2})\Big)\Big],
\end{aligned}$$

$$\begin{aligned}
A^{(3,4)} = {} & \delta^3(k-k_2)\Big[\delta^3(t'-k_1)\phi^{(3,4)*}(2'',\hat{1},3) + \delta^3(t'-k_3)\phi^{(3,4)*}(2'',1,\hat{3})\Big] \\
& + \delta^3(k-k_1)\Big[\delta^3(t'-k_2)\Big(2\phi^{(3,4)*}(\hat{2},1'',3) + \phi^{(3,4)*}(\hat{2},3,1'')\Big) \\
& + \delta^3(t'-k_3)\Big(2\phi^{(3,4)*}(2,1'',\hat{3}) + \phi^{(3,4)*}(2,\hat{3},1'')\Big)]\Big] \\
& + \delta^3(k-k_3)\Big[\delta^3(t'-k_1)\Big(\phi^{(3,4)*}(2,\hat{1},3'') + \phi^{(3,4)*}(2,3'',\hat{1})\Big) \\
& + \delta^3(t'-k_2)\Big(\phi^{(3,4)*}(\hat{2},1,3'') + \phi^{(3,4)*}(\hat{2},3'',1)\Big)\Big],
\end{aligned}$$

$$
\begin{aligned}
A^{(5)} = \delta^3(k-k_1)\Big[&\delta^3(t'-k_2)\Big(\phi^{(5)*}(1'',\hat{2},3)+\phi^{(5)*}(\hat{2},1'',3)\Big)\\
&+\delta^3(t'-k_3)\Big(\phi^{(5)*}(1'',2,\hat{3})+\phi^{(5)*}(2,1'',\hat{3})\Big)\Big]\\
&+\delta^3(k-k_2)\Big[\delta^3(t'-k_1)\Big(\phi^{(5)*}(\hat{1},2'',3)+\phi^{(5)*}(2'',\hat{1},3)\Big)\\
&+\delta^3(t'-k_3)\Big(\phi^{(5)*}(1,2'',\hat{3})+\phi^{(5)*}(2'',1,\hat{3})\Big)\Big],
\end{aligned}
$$

$$
\begin{aligned}
A^{(6)} = \delta^3(k-k_1)\Big[&\delta^3(t'-k_2)\Big(\phi^{(6)*}(1'',\hat{2},3)+\phi^{(6)*}(\hat{2},1'',3)\Big)\\
&+\delta^3(t'-k_3)\Big(\phi^{(6)*}(1'',2,\hat{3})+\phi^{(6)*}(2,1'',\hat{3})\Big)\Big]\\
&+\delta^3(k-k_2)\Big[\delta^3(t'-k_1)\Big(\phi^{(6)*}(\hat{1},2'',3)+\phi^{(6)*}(2'',\hat{1},3)\Big)\\
&+\delta^3(t'-k_3)\Big(\phi^{(6)*}(1,2'',\hat{3})+\phi^{(6)*}(2'',1,\hat{3})\Big)\Big],
\end{aligned}
\tag{36}
$$

where the quark coordinates are $\imath'' = (x, \boldsymbol{k}_\perp - \boldsymbol{q}_\perp)$, and $\hat{\imath} = (x', \boldsymbol{t}'_\perp + \boldsymbol{q}_\perp)$, $\delta^3(k-k_i) = \delta(x-x_i)\delta^2(\boldsymbol{k}_\perp - \boldsymbol{k}_{i\perp})$ and we used the notation $\delta^3(t'-k_i) = \delta(x'-x_i)\delta^2(\boldsymbol{t}'_\perp - \boldsymbol{k}_{i\perp})$. In the above equations, the complex conjugate only acts on the wave function $\psi^{(i)}$.

In Eq. (33), the contributions from the functions $A^{(1,2)}$ and $A^{(3,4)}$ describe the interference between $S$ and $P$ waves, while the terms with $A^{(5)}$ and $A^{(6)}$ correspond to the contribution from $P-D$ wave interference.

Similarly for the d-quark, one has

$$
\mathcal{F}^{\perp\, d} = B^{(1,2)}\phi^{(3,4)}(1,2,3) - B^{(3,4)}\phi^{(1,2)}(1,2,3) - B^{(5)}\phi^{(6)}(1,2,3) + B^{(6)}\phi^{(5)}(1,2,3), \tag{37}
$$

where the terms with $B^{(1,2)}$ and $B^{(3,4)}$ describe the interference between $S$ and $P$ waves, while the terms with $B^{(5)}$ and $B^{(6)}$ correspond to the contribution from $P-D$ wave interference. The explicit expression for these functions is

$$
\begin{aligned}
B^{(1,2)} = \delta^3(k-k_3)\Big[&\delta^3(t'-k_2)\phi^{(1,2)*}(\hat{2},1,3'')+\delta^3(t'-k_1)\phi^{(1,2)*}(2,\hat{1},3'')\Big]\\
&+\delta^3(k-k_1)\Big[\delta^3(t'-k_2)\Big(\phi^{(1,2)*}(\hat{2},1'',3)+\phi^{(1,2)*}(3,1'',\hat{2})\Big)\\
&+\delta^3(t'-k_3)\Big(\phi^{(1,2)*}(2,1'',\hat{3})+\phi^{(1,2)*}(\hat{3},1'',2)\Big)\Big],
\end{aligned}
$$

$$
\begin{aligned}
B^{(3,4)} = \delta^3(k-k_3)\Big[&\delta^3(t'-k_1)\phi^{(3,4)*}(2,\hat{1},3'')+\delta^3(t'-k_2)\phi^{(3,4)*}(\hat{2},1,3'')\Big]\\
&+\delta^3(k-k_2)\Big[\delta^3(t'-k_1)\Big(\phi^{(3,4)*}(2'',\hat{1},3)+\phi^{(3,4)*}(2'',3,\hat{1})\Big)\\
&+\delta^3(t'-k_3)\Big(\phi^{(3,4)*}(2'',1,\hat{3})+\phi^{(3,4)*}(2'',\hat{3},1)\Big)\Big],
\end{aligned}
$$

$$
\begin{aligned}
B^{(5)} = \delta^3(k-k_3)\Big[&\delta(t'-k_2)\Big(\phi^{(5)*}(1,\hat{2},3'')+\phi^{(5)*}(\hat{2},1,3'')\Big)\\
&+\delta(t'-k_1)\Big(\phi^{(5)*}(\hat{1},2,3'')+\phi^{(5)*}(2,\hat{1},3'')\Big)\Big],
\end{aligned}
$$

$$
\begin{aligned}
B^{(6)} = \delta^3(k-k_3)\Big[&\delta^3(t'-k_1)\Big(\phi^{(6)*}(\hat{1},2,3'')+\phi^{(6)*}(2,\hat{1},3'')\Big)\\
&+\delta^3(t'-k_2)\Big(\phi^{(6)*}(1,\hat{2},3'')+\phi^{(6)*}(\hat{2},1,3'')\Big)\Big].
\end{aligned}
\tag{38}
$$

In the above equations, the complex conjugate only acts on the wave function $\psi^{(i)}$.

Using the CQM expressions for the three-quark light cone amplitudes given in Sec. II, we obtain the following results for the Sivers function

$$f_{1T}^{\perp q}(x,\boldsymbol{k}_\perp^2) = -\frac{2}{3}g^2 M\frac{k^x+ik^y}{\boldsymbol{k}_\perp^2}\int\frac{\mathrm{d}^2\boldsymbol{q}_\perp}{(2\pi)^2}\frac{1}{\boldsymbol{q}_\perp^2}\int\mathrm{d}x'\int\mathrm{d}^2\boldsymbol{t}'_\perp\int d[1]d[2]d[3]\sqrt{x_1x_2x_3}$$
$$\times\delta(x-x_3)\delta^2(\boldsymbol{k}_\perp-\boldsymbol{k}_{3\perp})\delta(x'-x_1)\delta^2(\boldsymbol{t}'_\perp-\boldsymbol{k}_{1\perp})\,\psi^*(\{x'_i\},\{\boldsymbol{k}'_{i\perp}\})\,\psi(\{x_i\},\{\boldsymbol{k}_{i\perp}\})$$
$$\times 3\delta_{\tau_3\tau_q}\,\left\{\delta_{\tau_q 1/2}X^{00}(\{\boldsymbol{k}'_i\},\{\boldsymbol{k}_i\})+\frac{1}{3}[\delta_{\tau_q 1/2}+2\delta_{\tau_q -1/2}]X^{11}(\{\boldsymbol{k}'_i\},\{\boldsymbol{k}_i\})\right\}, \tag{39}$$

where the quark momenta in the final state are $(x'_3=x,\boldsymbol{k}'_{3\perp}=\boldsymbol{k}_{3\perp}-\boldsymbol{q}_\perp)$, $(x'_1=x',\boldsymbol{k}'_1=\boldsymbol{t}'_\perp+\boldsymbol{q}_\perp)$, $(x'_2=x_2,\boldsymbol{k}'_{2\perp}=\boldsymbol{k}_{2\perp})$. In Eq. (39), the functions $X^{00}$ and $X^{11}$ are given by

$$X^{00}(\{\boldsymbol{k}'_i\},\{\boldsymbol{k}_i\}) = \prod_{i=1}^{3}N^{-1}(\boldsymbol{k}'_i)N^{-1}(\boldsymbol{k}_i)(i\,B_{3x}+B_{3y})(A_1A_2+\boldsymbol{B}_1\cdot\boldsymbol{B}_2), \tag{40}$$

$$\begin{aligned}X^{11}(\{\boldsymbol{k}'_i\},\{\boldsymbol{k}_i\}) = &\prod_{i=1}^{3}N^{-1}(\boldsymbol{k}'_i)N^{-1}(\boldsymbol{k}_i)\\ &\times\frac{1}{3}\Big\{-(A_1A_2+\boldsymbol{B}_1\cdot\boldsymbol{B}_2)(iB_{3x}+B_{3y})\\ &\quad+2\boldsymbol{B}_1\cdot\boldsymbol{B}_3(iB_{2x}+B_{2y})+2\boldsymbol{B}_2\cdot\boldsymbol{B}_3(iB_{1x}+B_{1y})\\ &\quad+2i\Big[A_3A_1(iB_{2x}+B_{2y})+A_3A_2(iB_{1x}+B_{1y})\Big]\Big\},\end{aligned} \tag{41}$$

where

$$\begin{aligned}A_i &= (m+x'_iM'_0)(m+x_iM_0)+k'^y_ik^y_i+k'^x_ik^x_i,\\ B_{i,x} &= -(m+x'_iM'_0)k^y_i+(m+x_iM_0)k'^y_i,\\ B_{i,y} &= (m+x'_iM'_0)k^x_i-(m+x_iM_0)k'^x_i,\\ B_{i,z} &= k'^x_ik^y_i-k'^y_ik^x_i.\end{aligned} \tag{42}$$

## IV. BOER-MULDERS FUNCTION

The calculation of Sec. III can be repeated for the Boer-Mulders function, defined from the following quark correlation function

$$h_1^\perp(x,\boldsymbol{k}_\perp^2) = \epsilon^{ij}k^j\frac{M}{2\boldsymbol{k}_\perp^2}\int\frac{d\xi^-d^2\boldsymbol{\xi}_\perp}{(2\pi)^3}e^{-i(\xi^-k^+-\boldsymbol{\xi}_\perp\cdot\boldsymbol{k}_\perp)}\frac{1}{2}\sum_\Lambda\langle P\Lambda|\bar\psi(\xi^-,\boldsymbol{\xi}_\perp)\mathcal{L}^\dagger_\xi i\sigma^{i+}\gamma_5\mathcal{L}_0\psi(0)|P\Lambda\rangle\ . \tag{43}$$

Also in this case we expand the gauge link up to the next-to leading order, and following the same method we used in the calculation of the Sivers function, we find for the Boer-Mulders function

$$h_1^{\perp q}(x,\boldsymbol{k}_\perp^2) = -g^2\frac{k^x-ik^y}{\boldsymbol{k}_\perp^2}\frac{M}{2}\frac{1}{(2\pi)^{11}}\frac{1}{\sqrt{(2k^+)(2k_1^+)}}\int\frac{\mathrm{d}k_3^+\mathrm{d}^2\boldsymbol{k}_{3\perp}}{\sqrt{(2k_3^+)(2k_4^+)}}\int\mathrm{d}^2\boldsymbol{q}_\perp$$
$$\times\Big\{\frac{1}{\boldsymbol{q}_\perp^2}\sum_{\Lambda,\lambda_3}\sum_f\sum_{i.j}\sum_{k,l}T^a_{ij}T^b_{kl}\delta_{ab}\langle P\Lambda|b^{\dagger\,q}_{i,\uparrow}(k_1)b^q_{j,\downarrow}(k)b^{\dagger\,f}_{k,\lambda_3}(k_3)b^f_{l,\lambda_3}(k_4)|P\Lambda\rangle\Big\}, \tag{44}$$

where the quark momenta are defined as $k_1 = k - q$, $k_4 = k_3 - q$. The above equation corresponds to the diagram of Fig. 1 with $\lambda = -\lambda_1$ and $\lambda_4 = \lambda_3$ for the helicity of the interacting and spectator quarks, respectively, and $\Lambda = \Lambda'$ for the helicity of the nucleon in the initial and final states, i.e. the helicity is conserved at the quark-gluon vertex, while the helicity of the struck quark flips from the initial to the final state. Since the nucleon state has the same helicity in the initial and final state, the quark helicity flip must be compensated by a transfer of one unit of orbital angular momentum.

Inserting in Eq. (44) the light-cone wave-function amplitude decomposition of the nucleon state introduced in Sec. II, one finds the following results in terms of the amplitudes $\psi^{(i)}$

$$h_1^{\perp\, q}(x, \boldsymbol{k}_\perp^2) = \frac{2}{3} g^2 M \frac{k^x - ik^y}{\boldsymbol{k}_\perp^2} \int \frac{\mathrm{d}^2\boldsymbol{q}_\perp}{(2\pi)^2} \frac{1}{\boldsymbol{q}_\perp^2} \int \mathrm{d}x' \int \mathrm{d}^2\boldsymbol{t}'_\perp \int d[1]d[2]d[3] \sqrt{x_1 x_2 x_3}\, \mathcal{H}^{\perp\, q}, \tag{45}$$

where the function $\mathcal{H}^{\perp\, q}$ for the up quark is

$$\begin{aligned} \mathcal{H}^{\perp\, u} = &-C^{(1,2)} \tilde{\phi}^{(3,4)}(1,2,3) + \widetilde{C}^{(3,4)} \phi^{(1,2)}(1,2,3) - C^{(3,4)} \tilde{\phi}^{(6)}(1,2,3) \\ &+ \widetilde{C}^{(6)} \phi^{(3,4)}(1,2,3) + \widetilde{C}^{(1,2)} \phi^{(5)}(1,2,3) - C^{(5)} \tilde{\phi}^{(1,2)}(1,2,3), \end{aligned} \tag{46}$$

with

$$\begin{aligned} \tilde{\phi}^{(1,2)}(1,2,3) &= \psi^{(1)}(1,2,3) + i(k_1^x k_2^y - k_1^y k_2^x)\psi^{(2)}(1,2,3), \\ \tilde{\phi}^{(3,4)}(1,2,3) &= k_1^+ \psi^{(3)}(1,2,3) + k_2^+ \psi^{(4)}(1,2,3), \\ \tilde{\phi}^{(6)}(1,2,3) &= k_1^+ k_3^+ \psi^{(6)}(1,2,3) - k_1^+ k_2^+ \psi^{(6)}(1,3,2). \end{aligned} \tag{47}$$

In Eq. (46), the terms containing $C^{(1,2)}$ and $C^{(3,4)}$ describe the contribution from $S$ and $P$ wave interference, while $C^{(5)}$ and $C^{(6)}$ are associated with the $P - D$ wave interference terms. The explicit expression for these functions is

$$\begin{aligned} C^{(1,2)} = &\delta^3(k - k_2)\Big[\delta^3(t' - k_1)\Big(\phi^{(1,2)*}(\hat{1}, 3, 2'') + 2\phi^{(1,2)*}(2'', 3, \hat{1})\Big) \\ &+ \delta^3(t' - k_3)\Big(\phi^{(1,2)*}(1, \hat{3}, 2'') + 2\phi^{(1,2)*}(2'', \hat{3}, 1)\Big)\Big] \\ &+ \delta^3(k - k_3)\Big[\delta^3(t' - k_1)\phi^{(1,2)*}(3'', 2, \hat{1}) + \delta^3(t' - k_2)\phi^{(1,2)*}(3'', \hat{2}, 1)\Big], \end{aligned}$$

$$\begin{aligned} \tilde{C}^{(3,4)} = &\delta^3(k - k_1)\left[\delta^3(t' - k_2)\left(\tilde{\phi}^{(3,4)*}(3, \hat{2}, 1'') + 2\tilde{\phi}^{(3,4)*}(3, 1'', \hat{2})\right)\right. \\ &\left. + \delta^3(t' - k_3)\left(\tilde{\phi}^{(3,4)*}(\hat{3}, 2, 1'') + 2\tilde{\phi}^{(3,4)*}(\hat{3}, 1'', 2)\right)\right] \\ &+ \delta^3(k - k_3)\left[\delta^3(t' - k_1)\tilde{\phi}^{(3,4)*}(\hat{1}, 3'', 2) + \delta^3(t' - k_2)\tilde{\phi}^{(3,4)*}(\hat{1}, 3'', 2)\right], \end{aligned}$$

$$\begin{aligned} C^{(3,4)} = &\delta^3(k - k_1)\left[\delta^3(t' - k_2)\phi^{(3,4)*}(1'', \hat{2}, 3) + \delta^3(t' - k_3)\phi^{(3,4)*}(1'', 2, \hat{3})\right] \\ &+ \delta^3(k - k_2)\left[\delta^3(t' - k_1)\phi^{(3,4)*}(2'', \hat{1}, 3) + \delta^3(t' - k_3)\phi^{(3,4)*}(2'', 1, \hat{3})\right], \end{aligned}$$

$$\begin{aligned} \tilde{C}^{(6)} = &\delta^3(k - k_1)\left[\delta^3(t' - k_2)\left(\tilde{\phi}^{(6)*}(1'', \hat{2}, 3) + \tilde{\phi}^{(6)*}(\hat{2}, 1'', 3)\right)\right. \\ &\left. + \delta^3(t' - k_3)\left(\tilde{\phi}^{(6)*}(1'', 2, \hat{3}) + \tilde{\phi}^{(6)*}(2, 1'', \hat{3})\right)\right], \end{aligned}$$

$$\tilde{C}^{(1,2)} = \delta^3(k-k_1)\left[\delta^3(t'-k_2)\tilde{\phi}^{(1,2)*}(\hat{2},1'',3)+\delta^3(t'-k_3)\tilde{\phi}^{(1,2)*}(2,1'',\hat{3})\right]$$
$$+\delta^3(k-k_2)\left[\delta^3(t'-k_1)\tilde{\phi}^{(1,2)*}(\hat{1},2'',3)+\delta^3(t'-k_3)\tilde{\phi}^{(1,2)*}(1,2'',\hat{3})\right],$$

$$C^{(5)} = \delta^3(k-k_2)\Big[\delta^3(t'-k_1)\Big(\phi^{(5)*}(\hat{1},2'',3)+\phi^{(5)*}(2'',\hat{1},3)\Big)$$
$$+\delta^3(t'-k_3)\Big(\phi^{(5)*}(1,2'',\hat{3})+\phi^{(5)*}(2'',1,\hat{3})\Big)\Big]. \tag{48}$$

In the above equations, the complex conjugate only acts on the wave function $\psi^{(i)}$.

Analogously, the function $\mathcal{H}^{\perp}$ for the down quark is

$$\mathcal{H}^{\perp\, d} = D^{(1,2)}\tilde{\phi}^{(3,4)}(1,2,3) - \tilde{D}^{(3,4)}\phi^{(1,2)}(1,2,3) + D^{(3,4)}\tilde{\phi}^{(6)}(1,2,3)$$
$$-\tilde{D}^{(6)}\phi^{(3,4)}(1,2,3) + \tilde{D}^{(1,2)}\phi^{(5)}(1,2,3) - D^{(5)}\tilde{\phi}^{(1,2)}(1,2,3), \tag{49}$$

where the $S-P$ wave interference contribution comes from the terms proportional to $D^{(1,2)}$ and $D^{(3,4)}$, while the remaining two terms give the contribution from the interference of $P$ and $D$ waves. The function $D$ in Eq. (49) are defined as

$$D^{(1,2)} = \delta^3(k-k_3)\left[\delta^3(t'-k_1)\phi^{(1,2)*}(\hat{1},2,3'')+\delta^3(t'-k_2)\phi^{(1,2)*}(1,\hat{2},3'')\right],$$

$$\tilde{D}^{(3,4)} = \delta^3(k-k_3)\left[\delta^3(t'-k_1)\tilde{\phi}^{(3,4)*}(\hat{1},2,3'')+\delta^3(t'-k_2)\tilde{\phi}^{(3,4)*}(1,\hat{2},3'')\right],$$

$$D^{(3,4)} = \delta^3(k-k_3)\left[\delta^3(t'-k_1)\left(\phi^{(3,4)*}(3'',2,\hat{1})+\phi^{(3,4)*}(3'',\hat{1},2)\right)\right.$$
$$\left.+\,\delta^3(t'-k_2)\left(\phi^{(3,4)*}(3'',\hat{2},1)+\phi^{(3,4)*}(3'',1,\hat{2})\right)\right],$$

$$\tilde{D}^{(6)} = \delta^3(k-k_1)\left[\delta^3(t'-k_2)\left(\tilde{\phi}^{(6)*}(3,\hat{2},1'')+\tilde{\phi}^{(6)*}(\hat{2},3,1'')\right)\right.$$
$$\left.+\,\delta^3(t'-k_3)\left(\tilde{\phi}^{(6)*}(\hat{3},2,1'')+\tilde{\phi}^{(6)*}(2,\hat{3},1'')\right)\right],$$

$$\tilde{D}^{(1,2)} = \delta^3(k-k_2)\left[\delta^3(t'-k_1)\left(\tilde{\phi}^{(1,2)*}(\hat{1},2'',3)+\tilde{\phi}^{(1,2)*}(3,2'',\hat{1})\right)\right.$$
$$\left.+\,\delta^3(t'-k_3)\left(\tilde{\phi}^{(1,2)*}(1,2'',\hat{3})+\tilde{\phi}^{(1,2)*}(\hat{3},2'',1)\right)\right],$$

$$D^{(5)} = \delta^3(k-k_2)\Big[\delta^3(t'-k_1)\Big(\phi^{(5)*}(\hat{1},2'',3)+\phi^{(5)*}(3,2'',\hat{1})\Big)$$
$$+\delta^3(t'-k_3)\Big(\phi^{(5)*}(1,2'',\hat{3})+\phi^{(5)*}(\hat{3},2'',1)\Big)\Big]. \tag{50}$$

In the above equations, the complex conjugate only acts on the wave function $\psi^{(i)}$.

In the model for the three-quark light cone amplitudes introduced in Sec. II, we find the following explicit results

$$h_1^{\perp\, q}(x,\boldsymbol{k}_\perp^2) = \frac{2}{3}g^2 M\frac{k^x-ik^y}{\boldsymbol{k}_\perp^2}\int\frac{\mathrm{d}^2\boldsymbol{q}_\perp}{(2\pi)^2}\frac{1}{\boldsymbol{q}_\perp^2}\int\mathrm{d}x'\int\mathrm{d}^2\boldsymbol{t}'_\perp\int d[1]d[2]d[3]\sqrt{x_1x_2x_3}$$
$$\times\delta(x-x_3)\delta^2(\boldsymbol{k}_\perp-\boldsymbol{k}_{3\perp})\delta(x'-x_1)\delta^2(\boldsymbol{t}'_\perp-\boldsymbol{k}'_{1\perp})\,\psi^*(\{x'_i\},\{\boldsymbol{k}'_{i\perp}\})\,\psi(\{x_i\},\{\boldsymbol{k}_{i\perp}\})$$
$$\times 3\delta_{\tau_3\tau_q}\left\{\delta_{\tau_q 1/2}\tilde{X}^{00}(\{\boldsymbol{k}'_i\},\{\boldsymbol{k}_i\})+\frac{1}{3}[\delta_{\tau_q 1/2}+2\delta_{\tau_q -1/2}]\tilde{X}^{11}(\{\boldsymbol{k}'_i\},\{\boldsymbol{k}_i\})\right\}, \tag{51}$$

where the quark momenta in the final state are $(x_3' = x, \boldsymbol{k}'_{3\perp} = \boldsymbol{k}_{3\perp} - \boldsymbol{q}_\perp)$, $(x_1' = x', \boldsymbol{k}'_1 = \boldsymbol{t}'_\perp + \boldsymbol{q}_\perp)$, $(x_2' = x_2, \boldsymbol{k}'_{2\perp} = \boldsymbol{k}_{2\perp})$. In Eq. (51), the functions $\tilde{X}^{00}$ and $\tilde{X}^{11}$ are given by,

$$\tilde{X}^{00}(\{\boldsymbol{k}'_i\}, \{\boldsymbol{k}_i\}) = \prod_{i=1}^{3} N^{-1}(\boldsymbol{k}'_i) N^{-1}(\boldsymbol{k}_i) \Big[ (A_1 A_2 + \boldsymbol{B}_1 \cdot \boldsymbol{B}_2) \tilde{A}_3 \Big], \tag{52}$$

$$\begin{aligned} \tilde{X}^{11}(\{\boldsymbol{k}'\}, \{\boldsymbol{k}\})\Big) = \prod_{i=1}^{3} N^{-1}(\{\boldsymbol{k}'_i\}) N^{-1}(\{\boldsymbol{k}_i\}) \\ \times \frac{1}{3} \Big[ (3A_1 A_2 - \boldsymbol{B}_1 \cdot \boldsymbol{B}_2) \tilde{A}_3 + 2(A_1 B_{2,x} + A_2 B_{1,x}) \tilde{B}_{3,x} \\ + 2(A_1 B_{2,y} + A_2 B_{1,y}) \tilde{B}_{3,y} + 2(A_1 B_{2,z} + A_2 B_{1,z}) \tilde{B}_{3,z} \Big], \end{aligned} \tag{53}$$

where the functions $A_i$ and $\boldsymbol{B}_i$ are defined in Eq. (42), and

$$\begin{aligned} \tilde{A}_3 &= (m + x_3 M_0)(k_3'^x + i k_3'^y) - (m + x_3' M_0')(k_3^x + i k_3^y), \\ \tilde{B}_3^x &= -i(m + x_3' M_0')(m + x_3 M_0) + i(k_3'^x + i k_3'^y)(k_3^x + i k_3^y), \\ \tilde{B}_3^y &= (m + x_3' M_0')(m + x_3 M_0) + (k'_{3,x} + i k'_{3y})(k_3^x + i k_3^y), \\ \tilde{B}_3^z &= i(m + x_3' M_0')(k_3^x + i k_3^y) + i(m + x_3 M_0)(k_3'^x + i k_3'^y). \end{aligned} \tag{54}$$

## V. RESULTS AND DISCUSSION

The formalism described in the previous sections is applied in the following to a specific CQM, adopting a power-law form for the momentum-dependent part of the light-cone wave function, i.e.

$$\psi(\{x_i, \boldsymbol{k}_{i\perp}\}) = \frac{N'}{(M_0^2 + \beta^2)^\gamma}, \tag{55}$$

with $N'$ a normalization factor. In Eq. (55), the scale $\beta$, the parameter $\gamma$ for the power-law behaviour, and the quark mass $m$ are taken from Ref. [78], i.e., $\beta = 0.607$ GeV, $\gamma = 3.4$ and $m = 0.267$ GeV. According to the analysis of Ref. [79] these values lead to a very good description of many baryonic properties. The same parametrization of the momentum dependent part of the LCWF in Eq. (55) has been successfully applied also in recent works for the calculation of the electroweak properties of the nucleon [68], GPDs [26, 35, 64–66] and T-even TMDs [44, 70].

In order to fix the coupling constant appearing in Eqs. (33) and (45), we need to determine the hadronic scale of the model. This is achieved in a model independent way following the prescription of Ref. [80], by matching the value of the momentum fraction carried by the valence quarks, as computed in the model, with that obtained evolving backward the value experimentally determined at large $Q^2$. The strong coupling constant $\alpha_S(Q^2)$ entering the evolution code at NLO is computed by solving the NLO transcendental equation numerically,

$$\ln \frac{Q^2}{\Lambda^2_{\rm NLO}} - \frac{4\,\pi}{\beta_0\,\alpha_s} + \frac{\beta_1}{\beta_0^2} \ln \left[ \frac{4\,\pi}{\beta_0\,\alpha_s} + \frac{\beta_1}{\beta_0^2} \right] = 0\,, \tag{56}$$

as obtained from the renormalization group analysis [80, 81]. It differs from the more familiar expression

$$\frac{\alpha_s(Q^2)}{4\pi} = \frac{1}{\beta_0 \ln(Q^2/\Lambda^2_{\rm NLO})} \left( 1 - \frac{\beta_1}{\beta_0^2} \frac{\ln\ln(Q^2/\Lambda^2_{\rm NLO})}{\ln(Q^2/\Lambda^2_{\rm NLO})} \right), \tag{57}$$

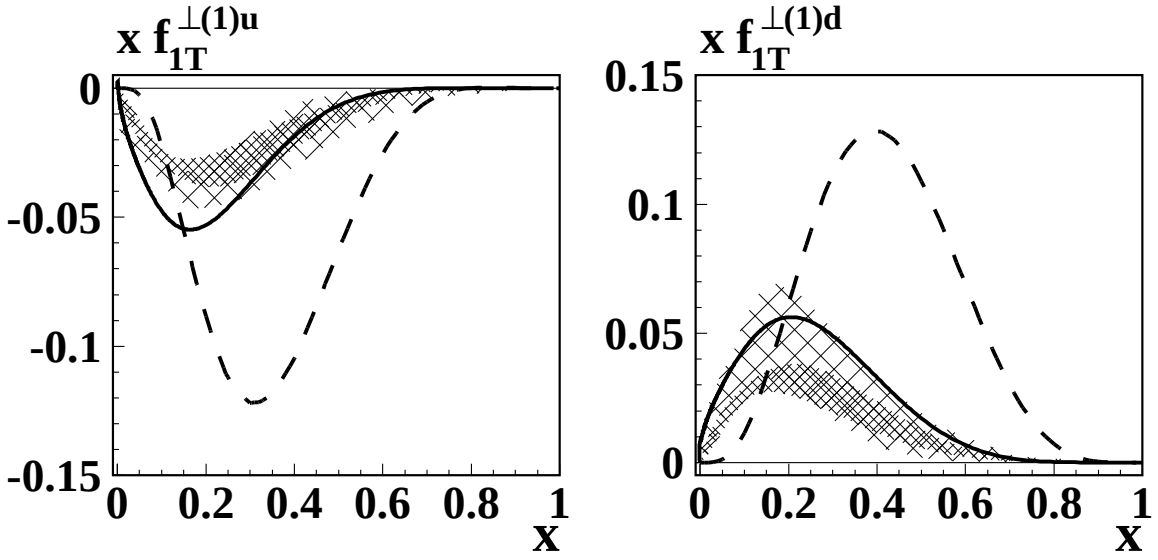


FIG. 2. Results for the first transverse-momentum moment of the Sivers function, for up (left) and down (right) quark, as function of $x$. The dashed curves show the results at the hadronic scale of the model $\mu_0^2 = 0.094$ GeV$^2$, and the solid curves correspond to the results after NLO evolution to $Q^2 = 2.5$ GeV$^2$, using the evolution pattern of the unpolarized parton distribution. The lighter and darker shaded areas are the uncertainty bands due to the statistical error of the parametrizations of Ref. [50] and Ref. [30, 54], respectively. Both parametrizations refer to an average scale of $Q^2 = 2.5$ GeV$^2$.

valid only in the limit $Q^2 \gg \Lambda^2_{\rm NLO}$, where $\Lambda_{\rm NLO}$ is the so-called QCD scale parameter. The hadronic scale, $\mu_0^2$, consistent with the presence of valence degrees of freedom only is $\mu_0^2 = 0.094$ GeV$^2$, with $\Lambda_{\rm NLO} = 0.248$ GeV. This corresponds to a value of the strong coupling constant in Eq. (56) $\alpha_S(\mu_0^2)/(4\pi) = g^2/(4\pi)^2 = 0.14$, and is consistent with the analysis of Refs. [46–48] where a similar procedure was adopted.

The first transverse-momentum moments of the Sivers and Boer-Mulders functions are shown in Figs. 2 and 3, using the definition

$$j^{(1)}(x) = \int {\rm d}^2\boldsymbol{k}_\perp \frac{\boldsymbol{k}_\perp^2}{2M^2} j(x, \boldsymbol{k}_\perp^2), \tag{58}$$

with $j = f_{1T}^{\perp q}$ and $j = h_1^\perp$, respectively. In the figures the dashed curves correspond to the results at the hadronic scale of the model $\mu_0^2$, while the solid curves are obtained by applying a NLO evolution to $Q^2 = 2.5$ GeV$^2$, assuming for the first transverse-momentum moment of the Sivers function the same anomalous dimension of the unpolarized parton distribution and for the first transverse-momentum moment of the Boer-Mulders the evolution pattern of the chiral-odd transversity distribution. Although these are not the exact evolution patterns, this is the standard procedure adopted so far in model calculations [45–48] and parametrizations [30, 50, 54] of the T-odd TMDs, since the exact evolution equations are still under study [17, 82–86] and evolution codes for these distributions are not yet available.

For the Sivers function in Fig. 2 we also show the results from recent parametrizations, valid at an average scale of $Q^2 = 2.5$ GeV$^2$, obtained from a fit to available experimental data on transverse single spin asymmetries for pion and kaon in semi-inclusive deep inelastic scattering. In particular, the darker shaded area represents the uncertainty due to the statistical errors in the parametrization of Ref. [50], while the lighter shaded area corresponds to the same for Ref. [30, 54]. The model predictions for the contribution of $u$ and $d$ quarks are of the same order of magnitude and opposite sign, and after evolution are well compatible with the phenomenological parametrizations. The effects of the evolution are crucial to reproduce the position of the peak at $x \approx 0.2$ for both the $u$ and $d$ quark distributions, and to rescale the magnitude of the distributions within the range of the parametrizations.

A non trivial constraint in model calculations of the Sivers function is given by the Burkardt sum rule [87]

$$\sum_{q=u,\,d,\,s,\,g,\cdots} \int \mathrm{d}x\, f_{1T}^{\perp\,(1)\,q}(x, \boldsymbol{k}_\perp^2) = 0 \ , \tag{59}$$

which corresponds to require that the net (summed over all partons) transverse momentum due to final-state interaction is zero [88]. Restricting the sum in Eq. (59) over the up- and down-quark contributions, our model calculation of the Sivers function reproduces exactly the sum rule.

In Fig. 3 we compare the model results for the absolute value of the Boer-Mulders function with phenomenological parametrizations obtained from recent fits to available experimental data. In particular, the dashed-dotted curve corresponds to the analysis of Refs. [89, 90] at the average scale of $Q^2 = 2.4$ GeV$^2$ of the HERMES [91] and COMPASS [92, 93] measurements of the $\cos 2\phi$ asymmetry in SIDIS, while the short-dashed curve shows the results of Refs. [94, 95] valid at $Q^2 \approx 1$ GeV$^2$, obtained from a fit to $pd$ [96] and $pp$ [97] Drell-Yan data measured by the E866/NuSea Collaboration, with the shaded area describing the variation ranges allowed by positivity bounds. We note that the available data do not allow yet a full fit of $h_1^\perp$ with its $x$ and $\boldsymbol{k}_\perp^2$ dependence and these phenomenological parametrizations are only first attempts to extract information on this distribution. Upcoming experimental SIDIS data also from JLab and plans for Drell-Yan experiments at GSI will play a crucial role to better constrain these analysis. Our model predictions after the "approximate" evolution to $Q^2 = 2.4$ GeV$^2$ are compatible with the phenomenological analysis of SIDIS data, reproducing both the peak position and the behaviour in $x$, while are at variance with the analysis of the Drell-Yan data. In particular we confirm the findings of Ref. [89] and the expectations from various theoretical analysis [48, 59, 98–100], predicting the same sign for both the up and down contributions, with the $u$ component of $h_1^\perp$ larger in magnitude than the corresponding component of $f_{1T}^\perp$ and the $d$ components of $h_1^\perp$ and $f_{1T}^\perp$ with approximately the same magnitude and opposite sign.

In Fig. 4 we show the decomposition of the Sivers and Boer-Mulders functions in the contributions from the different partial-wave amplitudes of the nucleon LCWF. The dashed curves correspond to the results from the interference of $S$ and $P$ waves, the dotted curves show the contribution from $P - D$ wave interference, and the solid curves are the total results, sum of all the partial wave contributions. The $S - P$ wave interference terms give the dominant contribution to the Sivers function of both $u$ and $d$ quarks, while the $P - D$ wave interference terms contribute at most by 20% of the total results. On the other side, the relative weight of the $P - D$ wave interference terms increases in the case of the Boer-Mulders function. It corresponds to 30% of the total results for the up-quark distribution

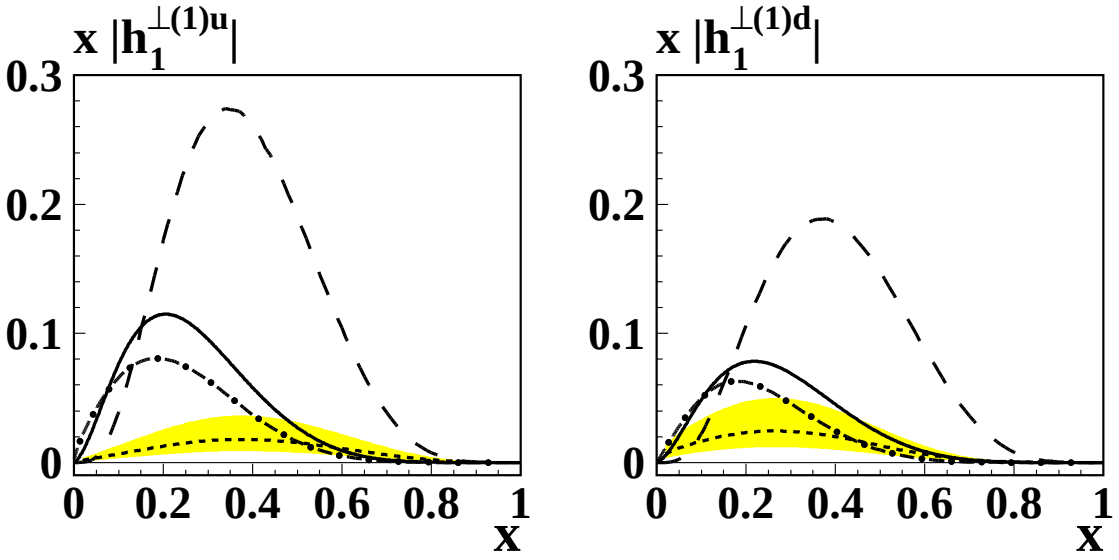


FIG. 3. Results for the first transverse-momentum moment of the Boer-Mulders function, for up (left) and down (right) quark, as function of $x$. The dashed curves show the results at the hadronic scale of the model $\mu_0^2 = 0.094$ GeV$^2$ and the solid curves correspond to the results after NLO evolution to $Q^2 = 2.5$ GeV$^2$, using the evolution pattern of the transversity distribution. The dashed-dotted curves are the results of the phenomenological parametrization of Refs. [89, 90] at the average scale of $Q^2 = 2.4$ GeV$^2$, and the short-dashed curves correspond the results of Refs. [94, 95] valid at $Q^2 \approx 1$ GeV$^2$, with the shaded area describing the variation ranges allowed by positivity bounds.

and becomes the dominant contribution in the case of down quark, reaching up to 60% of the total result. We also note that, contrary to the case of T-even TMDs [44], the assumption of SU(6) symmetry in the model does not imply any proportionality between the T-odd distributions of up and down quark. As outlined in Ref. [48], this is due to the fact that in the case of the T-odd functions one is using a two-body operator associated with FSI, while for the T-even TMDs the proportionality results from the calculation with a one-body operator.

In comparison with other model calculations, our light-cone model gives results which are similar in shape but significantly different in magnitude from the predictions in the non relativistic CQM of Refs. [46–48]. The main differences in this calculation can be traced back to the use of covariant quantization and non-relativistic wave functions. This implies a completely different helicity structure for the interacting and spectator quarks, which allows for overlap of $S-S$, $P-P$ and $S-P$ components of the wave functions of the initial and final proton state. Furthermore, the quark-gluon interaction vertex is treated non relativistically. Analogous discrepancies are evident in the comparison of our predictions with the results of the bag-model [47, 48, 58]. Here the calculation is fully relativistic, but the main difference comes from the use of covariant quantization which again leads to a different helicity structure for the quarks in the diagram of Fig. 1, with both helicity-conserving ($\lambda_3 = \lambda_4$) and helicity-flip ($\lambda_3 = -\lambda_4$) contributions at the quark-gluon vertex.

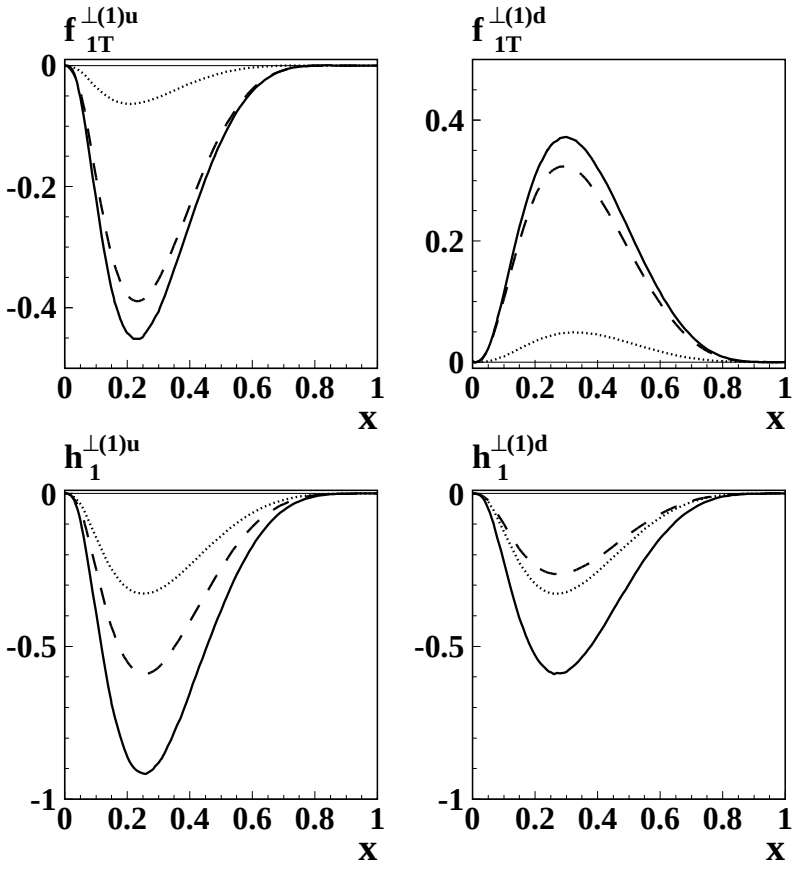


FIG. 4. Angular momentum decomposition of the first $\boldsymbol{k}_\perp$ moment of the Sivers function for the up (left panel ) and down (right panel) quark. The dashed curves show the contribution from the interference of $S$ and $P$ waves, and the dotted curves correspond to the contribution from the interference of $P$ and $D$ waves. The solid curves are the total results, sum of all the partial-wave contributions.

Finally, with respect to the diquark models of Refs. [40, 45] we have different magnitude and shape for both the Sivers and Boer Mulders functions. The different magnitude might be due to the different values for the quark-gluon coupling constant used in the calculations. Note however that our results are at variance with the calculations in the diquark models also for the relative magnitude between up- and down-quark contributions.

The dependence on $x$ and $\boldsymbol{k}_\perp^2$ of the Sivers and Boer-Mulders functions is shown in Figs. 5 and 6, respectively, for the separate up (left) and down (right) quark contributions.

The behaviour in $\boldsymbol{k}_\perp^2$ is very similar for the two distributions, and does not depend on the quark flavour. For the T-odd distributions there also exist positivity bounds which read [101]

$$\frac{k_\perp^2}{2M^2}\left[(f_{1T}^\perp)^2+(g_{1T}^\perp)^2\right] \leq \frac{1}{2}\left[(f_1)^2-(g_{1L})^2\right] \ , \tag{60}$$

$$\frac{k_\perp^2}{2M^2}\left[(h_1^\perp)^2+(h_{1L}^\perp)^2\right] \leq \frac{1}{2}\left[(f_1)^2-(g_{1L})^2\right] \ , \tag{61}$$

where the $(x, \boldsymbol{k}_\perp^2)$ dependence has been omitted, and $f_1$, $g_{1L}$, $g_{1T}^\perp$, and $h_{1L}^\perp$ are T-even TMDs. Using the results of the light-cone CQM for the T-even TMDs [44], we find that these

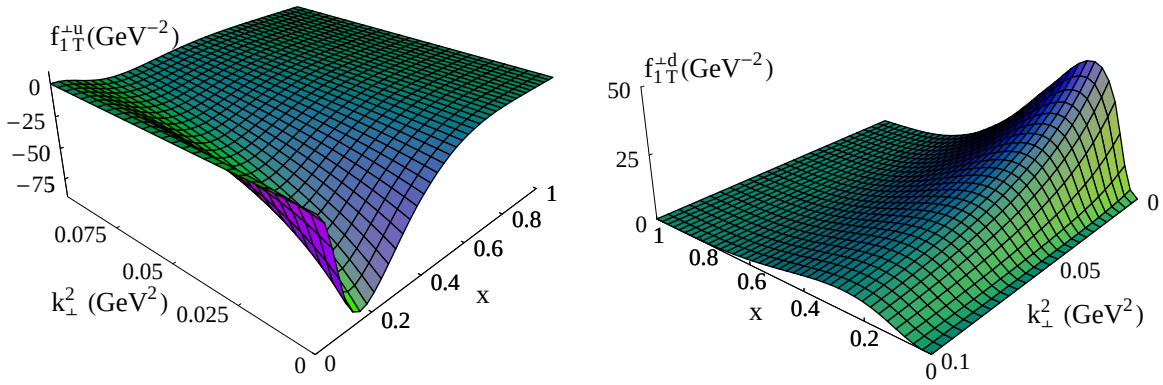


FIG. 5. The Sivers function $f_{1T}^{\perp}$ as function of $x$ and $\boldsymbol{k}_\perp^2$ for up (left panel) and down quark (right panel).

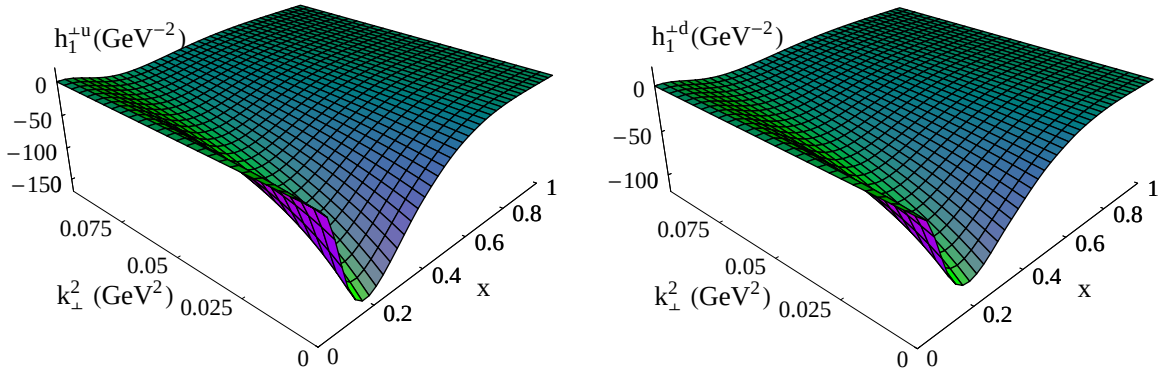


FIG. 6. The Boer-Mulders function $h_1^{\perp}$ as function of $x$ and $\boldsymbol{k}_\perp^2$ for up (left panel) and down quark (right panel).

constraints are satisfied.

The $\boldsymbol{k}_\perp^2$-dependence shown in Figs. 5 and 6 is definitely not of Gaussian form. However, following the exercise performed in Ref. [70] for the T-even distributions, it is interesting to compare the model predictions for the mean square transverse momenta with the results of the Gaussian model. We define the mean transverse momenta ($n = 1$) and the mean square transverse momenta ($n = 2$) for the TMD $j(x, \boldsymbol{k}_\perp^2)$ as follows

$$\langle k_{\perp,j}^n \rangle = \frac{\int \mathrm{d}x \int \mathrm{d}^2\boldsymbol{k}_\perp \; k_\perp^n \, j(x, \boldsymbol{k}_\perp^2)}{\int \mathrm{d}x \int \mathrm{d}^2\boldsymbol{k}_\perp \; j(x, \boldsymbol{k}_\perp^2)} \; , \tag{62}$$

where $k_\perp = |\boldsymbol{k}_\perp|$. The corresponding results for the T-odd distributions are shown in Table V. In the Gaussian model the following relation holds

$$\langle k_\perp^2 \rangle \stackrel{\text{Gauss}}{=} \frac{4}{\pi} \langle k_\perp \rangle^2 \; , \tag{63}$$

which implies that the ratio shown in the last column of Table V should be equal to one. The model results deviates from unit by 10%. We also note that the mean transverse momenta in Table V are quite small, much smaller than expected from phenomenological studies.

| TMD $j$ | $\langle k_\perp \rangle$ in GeV | | $\langle k_\perp^2 \rangle$ in GeV$^2$ | | $\frac{4\langle k_\perp \rangle^2}{\pi \langle k_\perp^2 \rangle}$ | |
|---|---|---|---|---|---|---|
| | up | down | up | down | up | down |
| $f_{1T}^\perp$ | 0.22 | 0.24 | 0.071 | 0.084 | 0.90 | 0.90 |
| $h_1^\perp$ | 0.23 | 0.24 | 0.077 | 0.080 | 0.90 | 0.91 |

TABLE I. The mean transverse momenta and the mean square transverse momenta of T-odd TMDs, as defined in Eq. (62), from the light-cone CQM. If the transverse momenta in the TMDs were Gaussian, then the result for the ratio in the third column would be unity, see text.

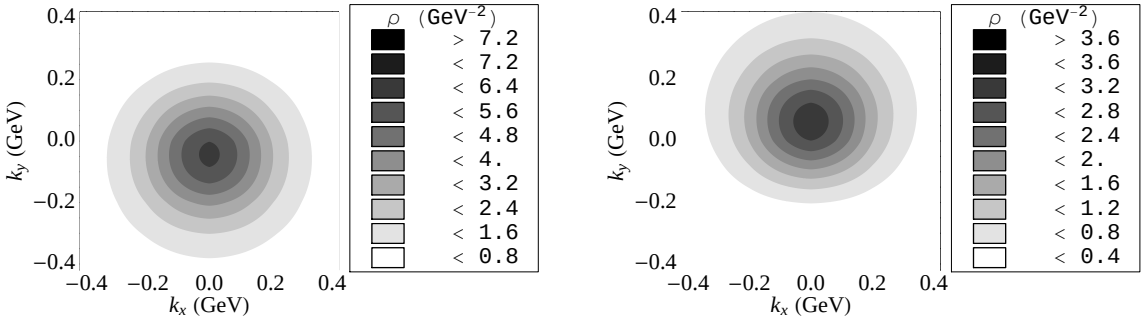


FIG. 7. Spin density in the transverse-momentum plane for unpolarized quarks in a transversely polarized nucleon. The left panel is for up quark, and the right panel for down quark.

This is due to the low scale of the model, and Sudakov effects are expected to make the $\boldsymbol{k}_\perp^2$ distributions larger when evolving to larger and experimentally relevant scale.

In Fig. 7, we show the spin density in the transverse-momentum space of unpolarized up (left panel) and down (right panel) quark in a transversely polarized nucleon, defined as

$$\rho^q_{f_{1T}^\perp}(\boldsymbol{k}_\perp) = \int \mathrm{d}x \frac{1}{2}\left[f_1^q(x, \boldsymbol{k}_\perp^2) + S_\perp^i \epsilon^{ij} k^j \frac{1}{M} f_{1T}^{\perp q}(x, \boldsymbol{k}_\perp^2)\right] \tag{64}$$

with $\boldsymbol{S}_\perp$ the nucleon transverse-polarization vector, and $f_1^q(x, k_\perp^2)$ the monopole distribution corresponding to spin densities for unpolarized quarks in an unpolarized target. When $\boldsymbol{S}_\perp$ points in the $\hat{x}$ direction, the dipole contribution related to the Sivers function introduces a large distortion on the monopole term, perpendicular to both the spin and the momentum of the proton and with ooposite sign for up and down quarks. The corresponding average transverse-momentum shift is defined as

$$\langle k^y \rangle^q_{f_{1T}^\perp} = \frac{\int \mathrm{d}^2\boldsymbol{k}_\perp k^y \rho^q_{f_{1T}^\perp}(\boldsymbol{k}_\perp)}{\int \mathrm{d}^2\boldsymbol{k}_\perp \rho^q_{f_{1T}^\perp}(\boldsymbol{k}_\perp)} \tag{65}$$

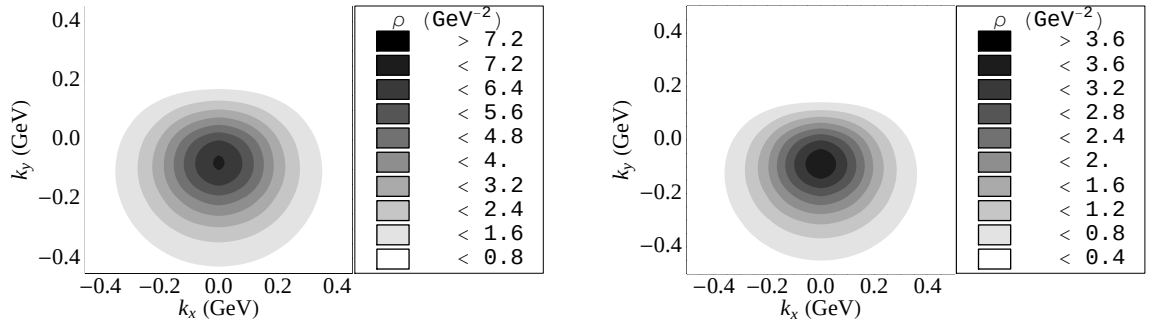


FIG. 8. Spin density in the transverse-momentum plane for transversely polarized quarks in an unpolarized nucleon. The left panel is for up quark, and the right panel for down quark.

and results

$$\langle k^y\rangle^u_{f_{1T}^\perp} = \frac{M}{2}\int \mathrm{d}x f_{1T}^{(1)\perp\, u}(x) = -70.31\,\mathrm{MeV}, \quad \langle k^y\rangle^d_{f_{1T}^\perp} = M\int \mathrm{d}x f_{1T}^{(1)\perp\, d}(x) = 140.62\,\mathrm{MeV}. \tag{66}$$

The fact that the absolute value of the average transverse momentum induced by the Sivers function is twice as large for $d$ quark than for $u$ quark is just a consequence of the Burkardt sum rule in Eq. (59). This intrinsic $\boldsymbol{k}_\perp$ shift is the analogous of the dipole deformation related to the GPD $E$ in impact-parameter space [63, 102]. Note that the LCWF overlap representation of $E$, for vanishing longitudinal momentum transfer, is given in terms of the same combinations of light-cone amplitudes parametrizing the Sivers function, but evaluated for different values of quark variables [64, 72]. The values for the average shifts in impact-parameter space within the present light-cone quark model were found $\langle b^y\rangle^u = \kappa^u/(2M) = 0.20\,\mathrm{fm}$ and $\langle b^y\rangle^d = \kappa^d/(M) = -0.33\,\mathrm{fm}$ [67], where $\kappa^q$ is the quark contribution to the proton anomalous magnetic moment.

Analogously, the spin density of transversely polarized quarks and unpolarized nucleon is related to the Boer-Mulders effect by

$$\rho^q_{h_1^\perp}(\boldsymbol{k}_\perp, \boldsymbol{s}_\perp) = \int \mathrm{d}x \frac{1}{2}\left[f_1^q(x,\boldsymbol{k}_\perp^2) + s^i\epsilon^{ij}k^j\frac{1}{M}h_1^{q\,\perp}(x,k_\perp^2)\right], \tag{67}$$

where $\boldsymbol{s}_\perp$ is the quark transverse-polarization vector. In Fig. 8 we show the spin density for quark polarization in the $\hat{x}$ direction. Since the Boer-Mulders function is negative for both up and down quarks, the sideway shift is always in the positive $\hat{y}$ direction. The corresponding average dipole distortion is

$$\langle k^y\rangle^u_{h_1^\perp} = \frac{M}{2}\int \mathrm{d}x h_1^{(1)\perp\, u}(x) = -159.40\,\mathrm{MeV}, \quad \langle k^y\rangle^d_{h_1^\perp} = M\int \mathrm{d}x h_1^{(1)\perp\, d}(x) = -215.73\,\mathrm{MeV}. \tag{68}$$

Although the Boer-Mulders function is smaller in magnitude for down quark than for up quark, one observes that the average sideways distortion for down quark is stronger. This is

because the monopole distribution related to $f_1^q$ is twice as large for up quarks as for down quarks, therefore adding the dipole contributions results in a more pronounced distortion for down quarks than for up quarks. The corresponding dipole distribution in impact-parameter space is described by the chiral odd GPDs $E_T + 2\tilde{H}_T$. As found in Ref. [66], these GPDs for zero longitudinal momentum transfer are given by the same combination of LCWFs which enter $h_{1T}^{\perp}$, but at different kinematics. The corresponding average distortion in impact-parameter space is proportional to tensor anomalous magnetic moment $\kappa_T^q$, and in the present light-cone quark model is given by $\kappa_T^u/(2M) = 0.42\,\mathrm{fm}$ and $\kappa_T^d/(M) = 0.55\,\mathrm{fm}$ for up and down quark, respectively [67].

## VI. CONCLUSIONS

In this paper we have investigated the naive-time-reversal-odd quark distributions, the quark Sivers and Boer-Mulders functions, in a light-cone quark model. The final-state interaction effects are calculated by approximating the gauge link operator with a one-gluon exchange interaction. In this framework, we have derived the general formalism for the T-odd quark distributions in terms of overlap of light-cone wave function amplitudes describing the different orbital angular momentum components of the nucleon state. This model independent expressions are particularly suitable to emphasize the correlations of quark transverse momentum and transverse polarizations of the nucleon and of the quark. For numerical estimates, the nucleon light-cone wave-function has been constructed by assuming a light-cone constituent quark model with SU(6) spin-flavor symmetry and a momentum-dependent part which is spherically symmetric. Under this assumption the orbital angular momentum content of the wave function is fully generated by the Melosh rotations which boost the rest-frame spin into the light-cone. As a result, we found explicit expressions for the light-cone amplitudes which match the analytic structure expected from model-independent arguments [72–74]. The model dependence enters the choice of the momentum-dependent part of the light-cone wave function. In this work, we adopted a phenomenological description, by assuming a specific functional form with parameters fitted to hadronic structure constants. The same wave function was used to predict many other hadronic properties, providing a good description of available experimental data, and being able to capture the main features of the quark contribution to hadronic structure functions, like parton distributions [35], generalized parton distributions [64–67], nucleon form factors [68], and T-even transverse momentum dependent quark distributions [44, 70].
The corresponding results for the Sivers and Boer-Mulders function have been presented in this paper by showing the decomposition into the contributions from different orbital angular momentum components. Both functions require a transfer of one unit of orbital angular momentum between the initial and final states. In particular, the Sivers function for both up and down quark is dominated by the interference of $S$- and $P$-wave components, while the $P - D$ wave interference terms contribute at most by 20% of the total results. On the other side, the relative weight of the $P - D$ wave interference terms increases in the case of the Boer-Mulders function, in particular for the down-quark component. Furthermore, the model results for the Sivers function satisfy exactly the so-called Burkardt sum rule, which is a non-trivial constraint for model calculations and parametrizations.

In order to compare with phenomenological parametrizations obtained from a fit to available experimental data for semi-inclusive deep inelastic scattering and Drell-Yan processes, we evolved the model results to the experimental scale. Since the exact evolution equations

for the T-odd quark distributions are still under study, we used those evolution equations which seem most promising to be able to simulate the correct evolution. We evolved the first transverse-momentum moment of the Sivers function by means of the evolution pattern of the unpolarized parton distribution, while for the first transverse-momentum moment of the Boer-Mulders we used the evolution pattern of the transversity. After evolution, the model results are consistent with the available parametrizations, especially for the Sivers function. There is agreement between the signs of the various flavor components, and also for the magnitude and the position of the maxima in $x$. These findings encourage further phenomenological applications of the model to describe azimuthal asymmetries in hadronic reactions.

We also found that the $x$ and $\boldsymbol{k}_\perp^2$ dependence is similar for the Sivers and Boer-Mulders functions, and approximately independent on the quark flavor. In particular, the $\boldsymbol{k}_\perp^2$ is not of Gaussian form. However, it is worthwhile to evaluate the degree of approximation introduced by the Gaussian Ansatz within the model in the calculation of observables. This task is left for future applications of the model.

Finally, we discussed the spin densities in the transverse-momentum space related to the Sivers and Boer-Mulders effects, showing that they are consistent with the model results for the corresponding spin densities in the impact-parameter space described by generalized parton distributions.

## ACKNOWLEDGMENTS

B.P. is grateful to A. Bacchetta, F. Conti, A. Courtoy and M. Radici for discussions, and to the Nuclear Science Division of Lawrence Berkeley National Laboratory, where this work was initiated, for hospitality. This work was supported in part by the Research Infrastructure Integrating Activity "Study of Strongly Interacting Matter" (acronym HadronPhysics2, Grant Agreement n. 227431) under the Seventh Framework Programme of the European Community, by the Italian MIUR through the PRIN 2008EKLACK "Structure of the nucleon: transverse momentum, transverse spin and orbital angular momentum", and by the U.S. Department of Energy under contracts DE-AC02-05CH11231 and DE-AC02-76SF00515. We are grateful to RIKEN, Brookhaven National Laboratory and the U.S. Department of Energy (contract number DE-AC02-98CH10886) for providing the facilities essential for the completion of this work.

[1] R. N. Cahn, Phys. Lett. B **78**, 269 (1978).
[2] J. C. Collins, D. E. Soper and G. Sterman, Nucl. Phys. B **250**, 199 (1985).
[3] D. W. Sivers, Phys. Rev. D **41**, 83 (1990); Phys. Rev. D **43**, 261 (1991).
[4] A. V. Efremov, L. Mankiewicz and N. A. Tornqvist, Phys. Lett. B **284**, 394 (1992).
[5] J. C. Collins, Nucl. Phys. B **396**, 161 (1993).
[6] J. C. Collins, S. F. Heppelmann and G. A. Ladinsky, Nucl. Phys. B **420**, 565 (1994).
[7] A. Kotzinian, Nucl. Phys. B **441**, 234 (1995).
[8] P. J. Mulders and R. D. Tangerman, Nucl. Phys. B **461**, 197 (1996) [Erratum-ibid. B **484** (1997) 538].
[9] D. Boer and P. J. Mulders, Phys. Rev. D **57** (1998) 5780.
[10] D. Boer, R. Jakob and P. J. Mulders, Nucl. Phys. B **504**, 345 (1997).
[11] D. Boer, Phys. Rev. D **60**, 014012 (1999).
[12] S. J. Brodsky, D. S. Hwang and I. Schmidt, Phys. Lett. B **530**, 99 (2002); Nucl. Phys. B **642**, 344 (2002).
[13] J. C. Collins, Phys. Lett. B **536**, 43 (2002).
[14] A. V. Belitsky, X. Ji and F. Yuan, Nucl. Phys. B **656**, 165 (2003); X. D. Ji and F. Yuan, Phys. Lett. B **543**, 66 (2002);
D. Boer, P. J. Mulders and F. Pijlman, Nucl. Phys. B **667**, 201 (2003).
[15] A. Bacchetta, P. J. Mulders and F. Pijlman, Phys. Lett. B **595**, 309 (2004).
[16] W. Vogelsang and F. Yuan, Phys. Rev. D **72**, 054028 (2005);
[17] I. O. Cherednikov and N. G. Stefanis, Phys. Rev. D **77**, 094001 (2008); Nucl. Phys. B **802**, 146 (2008).
[18] V. Barone, A. Drago and P. G. Ratcliffe, Phys. Rept. **359**, 1 (2002).
[19] K. Goeke, A. Metz and M. Schlegel, Phys. Lett. B **618**, 90 (2005).
[20] A. Bacchetta, M. Diehl, K. Goeke, A. Metz, P. J. Mulders and M. Schlegel, JHEP **0702**, 093 (2007).
[21] U. D'Alesio and F. Murgia, Prog. Part. Nucl. Phys. **61**, 394 (2008).
[22] K. Goeke , M.V. Polyakov, and M. Vanderhaeghen, Prog. Part. Nucl. Phys. **47**, 401 (2001);
[23] M. Diehl, Phys. Rep. **388**, 41 (2003);
[24] X. Ji, Ann. Rev. Nucl. Part. Sci. **54**, 413 (2004);
[25] A.V. Belitsky and A.V. Radyushkin, Phys. Rep. **418**, 1 (2005);
[26] S. Boffi and B. Pasquini, Riv. Nuovo Cim. **30**, 387 (2007).
[27] J. C. Collins and D. E. Soper, Nucl. Phys. B **193**, 381 (1981) [Erratum-ibid. B **213**, 545 (1983)]; Nucl. Phys. B **194**, 445 (1982).
[28] X. D. Ji, J. P. Ma and F. Yuan, Phys. Rev. D **71**, 034005 (2005); Phys. Lett. B **597**, 299 (2004).
[29] J. C. Collins and A. Metz, Phys. Rev. Lett. **93**, 252001 (2004).
[30] J. C. Collins, A. V. Efremov, K. Goeke, S. Menzel, A. Metz and P. Schweitzer, Phys. Rev. D **73**, 014021 (2006).
[31] J. C. Collins *et al.*, Phys. Rev. D **73**, 094023 (2006).
[32] A. V. Efremov, K. Goeke and P. Schweitzer, Phys. Rev. D **73**, 094025 (2006).
[33] A. Kotzinian, B. Parsamyan and A. Prokudin, Phys. Rev. D **73**, 114017 (2006).
[34] S. J. Brodsky and F. Yuan, Phys. Rev. D **74**, 094018 (2006).

[35] B. Pasquini, M. Pincetti and S. Boffi, Phys. Rev. D **76**, 034020 (2007).
[36] S. Meissner, A. Metz and K. Goeke, Phys. Rev. D **76**, 034002 (2007).
[37] M. Anselmino, M. Boglione, U. D'Alesio, A. Kotzinian, F. Murgia, A. Prokudin and C. Turk, Phys. Rev. D **75**, 054032 (2007).
[38] M. Anselmino, M. Boglione, U. D'Alesio, A. Kotzinian, F. Murgia, A. Prokudin and S. Melis, Nucl. Phys. Proc. Suppl. **191**, 98 (2009).
[39] L. P. Gamberg, G. R. Goldstein and K. A. Oganessyan, Phys. Rev. D **67**, 071504 (2003).
[40] L. P. Gamberg, G. R. Goldstein and M. Schlegel, Phys. Rev. D **77**, 094016 (2008).
[41] A. Bacchetta, L.P. Gamberg, G.R. Goldstein, A. Mukherjee, Phys. Lett. B **659**, 234 (2008).
[42] H. Avakian, A. V. Efremov, K. Goeke, A. Metz, P. Schweitzer and T. Teckentrup, Phys. Rev. D **77**, 014023 (2008).
[43] H. Avakian, S. J. Brodsky, A. Deur and F. Yuan, Phys. Rev. Lett. **99**, 082001 (2007).
[44] B. Pasquini, S. Cazzaniga and S. Boffi, Phys. Rev. D **78**, 034025 (2008).
[45] A. Bacchetta, F. Conti and M. Radici, Phys. Rev. D **78**, 074010 (2008).
[46] A. Courtoy, F. Fratini, S. Scopetta and V. Vento, Phys. Rev. D **78** (2008) 034002.
[47] A. Courtoy, S. Scopetta and V. Vento, Phys. Rev. D **79**, 074001 (2009).
[48] A. Courtoy, S. Scopetta and V. Vento, Phys. Rev. D **80**, 074032 (2009).
[49] H. Avakian, A. V. Efremov, P. Schweitzer and F. Yuan, Phys. Rev. D **78**, 114024 (2008).
[50] M. Anselmino *et al.*, Eur. Phys. J. A **39** (2009) 89; M. Anselmino, M. Boglione, U. D'Alesio, A. Kotzinian, F. Murgia and A. Prokudin, Phys. Rev. D **71**, 074006 (2005); M. Anselmino, M. Boglione, U. D'Alesio, A. Kotzinian, F. Murgia and A. Prokudin, Phys. Rev. D **72**, 094007 (2005) [Erratum-ibid. D **72**, 099903 (2005)];
[51] S. Arnold, A. V. Efremov, K. Goeke, M. Schlegel and P. Schweitzer, arXiv:0805.2137 [hep-ph].
[52] A. V. Efremov, P. Schweitzer, O. V. Teryaev and P. Zavada, Phys. Rev. D **80**, 014021 (2009).
[53] J. She, J. Zhu and B. Q. Ma, Phys. Rev. D **79**, 054008 (2009).
[54] A. V. Efremov, K. Goeke, S. Menzel, A. Metz and P. Schweitzer, Phys. Lett. B **612**, 233 (2005).
[55] R. Jakob, P. J. Mulders and J. Rodrigues, Nucl. Phys. A **626**, 937 (1997); Proc. Int. Conf. on Perspectives in Hadronic Physics, S. Boffi, C. Ciofi degli Atti, M. Giannini, eds., (World Scientific Singapore, 1998), p. 320, arXiv:hep-ph/9707340.
[56] A. V. Efremov and P. Schweitzer, JHEP **0308**, 006 (2003).
[57] A. V. Efremov, K. Goeke and P. Schweitzer, Eur. Phys. J. C **32**, 337 (2003).
[58] F. Yuan, Phys. Lett. B **575**, 45 (2003).
[59] P. V. Pobylitsa, arXiv:hep-ph/0301236.
[60] A. V. Efremov, K. Goeke and P. Schweitzer, Eur. Phys. J. C **35**, 207 (2004).
[61] L. Gamberg and M. Schlegel, arXiv:0911.1964 [hep-ph].
[62] M. Burkardt, Nucl. Phys. A **735**, 185 (2004); Phys. Rev. D **66**, 114005 (2002); M. Burkardt and D. S. Hwang, Phys. Rev. D **69**, 074032 (2004).
[63] S. Meissner, A. Metz and M. Schlegel, JHEP **0908**, 056 (2009).
[64] S. Boffi, B. Pasquini and M. Traini, Nucl. Phys. B **649**, 243 (2003).
[65] S. Boffi, B. Pasquini and M. Traini, Nucl. Phys. B **680**, 147 (2004).
[66] B. Pasquini, M. Pincetti and S. Boffi, Phys. Rev. D **72**, 094029 (2005).
[67] B. Pasquini and S. Boffi, Phys. Lett. B **653**, 23 (2007).
[68] B. Pasquini, and S. Boffi, Phys. Rev. D **76**, 074011 (2007).
[69] S.J. Brodsky, H.-Ch. Pauli, S.S. Pinsky, Phys. Rept. **301**, 299 (1998).
[70] S. Boffi, A. V. Efremov, B. Pasquini and P. Schweitzer, Phys. Rev. D **79** (2009) 094012.

[71] S. J. Brodsky, B. Pasquini, B. Xiao and F. Yuan, arXiv:1001.1163 [hep-ph].
[72] X. Ji, J. P. Ma and F. Yuan, Nucl. Phys. B **652**, 383 (2003).
[73] M. Burkardt, X. Ji and F. Yuan, Phys. Lett. B **545**, 345 (2002).
[74] X. Ji, J.-P. Ma and F. Yuan, Eur. Phys. J. C **33**, 75 (2004); Phys. Rev. Lett. **90**, 241601 (2003).
[75] J. Franklin, Phys. Rev. **172**, 1807 (1968).
[76] S. Capstick, Phys. Rev. D **34**, 2809 (1986).
[77] H.J. Melosh, Phys. Rev. **D 9**, 1095 (1974).
[78] F. Schlumpf, doctoral thesis, University of Zurich, 1992; hep-ph/9211255.
[79] F. Schlumpf, J. Phys. G: Nucl. Part. Phys. **20**, 237 (1994); Phys. Rev. **D 47**, 4114 (1993); Erratum-*ibid.* **D 49**, 6246 (1993); S.J. Brodsky and F. Schlumpf, Phys. Lett. **B 329**, 111 (1994).
[80] B. Pasquini, M. Traini and S. Boffi, Phys. Rev. D **71**, 034022 (2005).
[81] T. Weigl and W. Melnitchouk, Nucl. Phys. B **465**, 267 (1996); M. Traini, A. Mair, A. Zambarda and V. Vento, Nucl. Phys. A **614**, 472 (1997).
[82] F. A. Ceccopieri and L. Trentadue, Phys. Lett. B **636**, 310 (2006); Phys. Lett. B **660**, 43 (2008).
[83] Z. B. Kang and J. W. Qiu, Phys. Rev. D **79**, 016003 (2009).
[84] J. Zhou, F. Yuan and Z. T. Liang, Phys. Rev. D **79**, 114022 (2009).
[85] W. Vogelsang and F. Yuan, Phys. Rev. D **79**, 094010 (2009).
[86] V. M. Braun, A. N. Manashov and J. Rohrwild, Nucl. Phys. B **826**, 235 (2010).
[87] M. Burkardt, Phys. Rev. D **69** (2004) 091501; Phys. Rev. D **69** (2004) 057501 .
[88] M. Burkardt, Nucl. Phys. Proc. Suppl. **141**, 86 (2005).
[89] V. Barone, A. Prokudin and B. Q. Ma, Phys. Rev. D **78** (2008) 045022.
[90] V. Barone, S. Melis and A. Prokudin, arXiv:0912.5194 [hep-ph].
[91] F. Giordano and R. Lamb [On behalf of the HERMES Collaboration], AIP Conf. Proc. **1149**, 423 (2009).
[92] W. Kafer [COMPASS Collaboration], arXiv:0808.0114 [hep-ex].
[93] A. Bressan [COMPASS Collaboration], arXiv:0907.5511 [hep-ex].
[94] B. Zhang, Z. Lu, B. Q. Ma and I. Schmidt, Phys. Rev. D **78**, 034035 (2008); Phys. Rev. D **77** (2008) 054011.
[95] Z. Lu and I. Schmidt, arXiv:0912.2031 [hep-ph].
[96] L. Y. Zhu *et al.* [FNAL-E866/NuSea Collaboration], Phys. Rev. Lett. **99**, 082301 (2007).
[97] L. Y. Zhu *et al.* [FNAL E866/NuSea Collaboration], Phys. Rev. Lett. **102**, 182001 (2009).
[98] M. Burkardt, Phys. Rev. D **72**, 094020 (2005).
[99] M. Burkardt and B. Hannafious, Phys. Lett. B **658**, 130 (2008).
[100] M. Gockeler *et al.* [QCDSF Collaboration and UKQCD Collaboration], Phys. Rev. Lett. **98** (2007) 222001.
[101] A. Bacchetta, M. Boglione, A. Henneman and P. J. Mulders, Phys. Rev. Lett. **85**, 712 (2000).
[102] M. Diehl and Ph. Hägler, Eur. Phys. J. C **44**, 87 (2005).